

การศึกษาอิทธิพลของอนุภาคทองคำในระดับนาโนเมตรต่อการแสดงออกของยีนในไมโทคอนเดรียของ

HeLa cells



นางสาวอรุณา กำเนิดสินธุ์

วิทยานิพนธ์นี้เป็นส่วนหนึ่งของการศึกษาตามหลักสูตรปริญญาวิทยาศาสตรมหาบัณฑิต


สาขาวิชาวิทยาศาสตร์การแพทย์

คณะแพทยศาสตร์ จุฬาลงกรณ์มหาวิทยาลัย

ปีการศึกษา 2552

ลิขสิทธิ์ของจุฬาลงกรณ์มหาวิทยาลัย

INFLUENCE OF GOLD NANOPARTICLES ON MITOCHONDRIAL GENE EXPRESSION IN
HELA CELLS.



Miss Oraya Kamnerdsin

A Thesis Submitted in Partial Fulfillment of the Requirements
for the Degree of Master of Science Program in Medical Sciences

Faculty of Medicine


Chulalongkorn University

Academic Year 2009

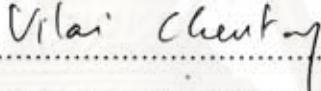
Copyright of Chulalongkorn University

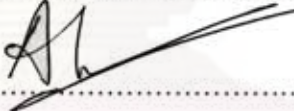
Thesis Title INFLUENCE OF GOLD NANOPARTICLES ON MITOCHONDRIAL
GENE EXPRESSION IN HELA CELLS.
By Miss Oraya Kamnerdsin
Field of Study Medical Science
Thesis Advisor Amornpun Sereemasapun, M.D., Ph.D.

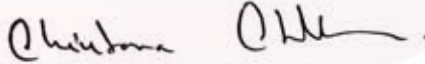
Accepted by the Faculty of Medicine, Chulalongkorn University in Partial
Fulfillment of the Requirements for the Master's Degree

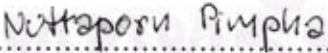

..... Dean of the Faculty of Medicine
(Associate Professor Adisorn Patradul, M.D.)

THESIS COMMITTEE


..... Chairman
(Associate Professor Vilai Chentanez, M.D.)


..... Thesis Advisor
(Amornpun Sereemasapun, M.D., Ph.D.)


..... Thesis Co-advisor
(Associate Professor Chintana Chirathaworn, Ph.D.)


..... External Examiner
(Nuttaporn Pimpha, Ph.D.)

ศูนย์วิจัยทางการแพทย์
จุฬาลงกรณ์มหาวิทยาลัย

อรญา กำเนิดสินธุ์: การศึกษาอิทธิพลของอนุภาคทองคำในระดับนาโนเมตรต่อการแสดงออกของยีนไมโทคอนเดรียของ HeLa cells. (INFLUENCE OF GOLD NANOPARTICLES ON MITOCHONDRIAL GENE EXPRESSION IN HELA CELLS.) อ. ที่ปริกษาวิทยานิพนธ์หลัก : นพ.ดร. อมรพันธุ์ เสรีมาศพันธุ์, 66 หน้า.

อนุภาคทองคำระดับนาโนเมตร (Gold nanoparticle, AuNP) เป็นอนุภาคของโลหะในระดับนาโนเมตรที่มีความเสถียรสูงชนิดหนึ่ง ในปัจจุบันอนุภาคทองคำในระดับนาโนเมตรถูกนำมาประยุกต์ใช้เป็นอุปกรณ์ตรวจวัดสารทางชีวภาพที่มีความจำเพาะสูง อุปกรณ์นำส่งยาหรือยีน และ contrast agents เป็นต้น โดยอาศัยความสามารถในการปรับปรุงพื้นผิวของอนุภาคทองคำในระดับนาโนเมตรด้วยสารชีวโมเลกุลต่างๆ เช่น ดีเอ็นเอ, โปรตีน, คาร์โบไฮเดรต, ยา หรือ สีเรืองแสงฟลูออเรสเซนต์ เป็นต้น ในขณะเดียวกัน ผลการศึกษาที่ผ่านมาถึงความเป็นพิษของอนุภาคทองคำในระดับนาโนเมตรพบว่ายังมีความขัดแย้งกันอยู่ ดังนั้นงานวิจัยนี้จึงทำการศึกษาผลของอนุภาคทองคำในระดับนาโนเมตรต่อ HeLa cells ทั้งผลต่อความมีชีวิตรอดของเซลล์ ลักษณะรูปร่างของเซลล์และอวัยวะต่างๆ ในเซลล์ การเคลื่อนที่ของอนุภาคทองคำในระดับนาโนเมตรในเซลล์ รวมถึงการแสดงออกของยีนไมโทคอนเดรีย

การศึกษาทำโดยบ่มเซลล์กับอนุภาคทองคำในระดับนาโนเมตรที่ความเข้มข้นต่างๆ เป็นเวลา 1, 2 และ 3 วัน เมื่อครบตามเวลาที่กำหนด เก็บเซลล์มาศึกษาลักษณะรูปร่างของเซลล์และอวัยวะต่างๆ ในเซลล์ ตำแหน่งของอนุภาคทองคำในระดับนาโนเมตร โดยใช้กล้องจุลทรรศน์และกล้องจุลทรรศน์อิเล็กตรอน และศึกษาความมีชีวิตรอดของเซลล์ โดย MTT assay นอกจากนี้นำเซลล์มาสกัดอาร์เอ็นเอและนำไปทำ RT-PCR เพื่อดูการแสดงออกของยีนไมโทคอนเดรีย จากการศึกษาพบว่าอนุภาคทองคำในระดับนาโนเมตรความเข้มข้น 100 $\mu\text{g}/\text{mL}$ มีผลลดความมีชีวิตรอดของเซลล์ และทำให้ลักษณะรูปร่างของเซลล์เปลี่ยนแปลงไป ขณะเดียวกันพบว่าอนุภาคทองคำในระดับนาโนเมตรสามารถผ่านเยื่อหุ้มเซลล์ได้ โดยถูกห่อหุ้มอยู่ใน endosome ทั้งนี้อนุภาคทองคำในระดับนาโนเมตรจะรวมกลุ่มกันอยู่ภายในไซโตพลาสซึมเท่านั้น โดยไม่พบว่าอนุภาคทองคำในระดับนาโนเมตรในอวัยวะอื่นๆ ของเซลล์ นอกจากนี้พบว่าการแสดงออกของยีนไมโทคอนเดรีย ไม่มีการเปลี่ยนแปลงเมื่อได้รับ อนุภาคทองคำในระดับนาโนเมตร

สาขาวิชา วิทยาศาสตร์การแพทย์
ปีการศึกษา 2552

ลายมือชื่อนิสิต.....อรญา กำเนิดสินธุ์.....
ลายมือชื่อ อ.ที่ปริกษาวิทยานิพนธ์หลัก.....

5074866830 : MAJOR MEDICAL SCIENCES

KEYWORDS: GOLD NANOPARTICLES/CYTOTOXICITY/CELL VIABILITY/MITOCHONDRIA

ORAYA KAMNERDSIN: INFLUENCE OF GOLD NANOPARTICLES ON

MITOCHONDRIAL GENE EXPRESSION IN HELA CELLS. THESIS ADVISOR:

AMORN PUN SEREEMASPUN, M.D., Ph.D., 66 pp.

Gold nanoparticle (AuNP) is a stable and inert metal nanoparticle. AuNP has been used as biosensors, drug/gene delivery devices and contrast agents because of its surface functionalization. AuNP can be tailored with biomolecules such as DNA, protein, carbohydrate, drug and fluorescent dye. However, the previous studies show that AuNP toxicity data are conflicted. Hence, this study aims to evaluate the toxicity of AuNP on HeLa cells including cell viability, cellular/intracellular organelles morphology, AuNP localization and mitochondrial gene expression.

HeLa cells were incubated with various concentrations of gold nanoparticles for 1, 2 and 3 days. Cells were evaluated for cellular/intracellular organelles morphology, localization of AuNP, cell viability and mitochondrial gene expression using light microscope, transmission electron microscope MTT assay and RT-PCR, respectively. This study demonstrated that 100 $\mu\text{g}/\text{mL}$ AuNP decreased cell viability and affected cellular morphology. However, intracellular organelles morphology was not irregular. The aggregated AuNPs were mainly entrapped in the endosome and localized in the cytoplasm. Furthermore, the mitochondrial gene expression level was unchanged.

Field of study: Medical Sciences

Academic year: 2008

Student's signature: ...Oraya Kamnerdsin.....

Advisor's signature:.....

ACKNOWLEDGEMENTS

First of all, I would like to thank my advisor, Dr. Amornpun Sereemaspun, Anatomy Department, Faculty of Medicine, Chulalongkorn University for leading me to the world of nanotechnology. His enlightening ideas are always support me during the course. He had been very supportive and patient with me during the thesis.

I would like to deeply thank my co-advisor, Associate Professor Dr. Chintana Chirathaworn, Division of Immunology, Microbiology Department, Faculty of Medicine, Chulalongkorn University for her very useful comments and for allowing me to work at her laboratory. She has wide knowledge in both biology, and all. Discussions with her have provided me a much deeper understanding.

I would like to thank my thesis committee, Associate Professor Dr. Vilai Chentanez, the Associate Dean of Graduate Affairs, Faculty of Medicine, Chulalongkorn University, for kindly accepting to be the chairman of my thesis committee. I wish to thank Dr. Nuttaporn Pimpha, National Nanotechnology Center for being on my thesis committee.

Then, I would like to thank Professor Dr. Aphiwat Muthirangura, Anatomy Department, Faculty of Medicine, Chulalongkorn University for his continuous support, providing good suggestions and allowing me to work at his laboratory. My thankfulness is also extended to Associate Professor Dr. Supang Maneesri le Grand and Ms.Penpan Nualboonma, Electron Microscope Laboratory, Chulalongkorn University for teaching and providing the TEM technique. Your help is deeply appreciated.

At least but not the last, I wish to thank Chulalongkorn University Medical Research Center (Chula MRC) for providing some research facilities. I would like to thank my colleagues from Nanobiomedicine Laboratory, Mr.Pattadons Sukkapan, Ms.Alisa Lowanitchapat and members in Center for Excellent in Genetics of Cancer and Human Diseases who discuss questions and kindly teach me on molecular technique. Finally, I would like to thank my family for their endless love, believing and continuous support during my study.

CONTENTS

	Page
ABSTRACT (THAI).....	iv
ABSTRACT (ENGLISH).....	v
ACKNOWLEDGEMENTS.....	vi
CONTENTS.....	vii
LIST OF TABLES.....	x
LIST OF FIGURES.....	xi
LIST OF ABBREVIATIONS.....	xiii
CHAPTER I BACKGROUND.....	1
CHAPTER II LITERRATURE REVIEW.....	5
2.1 Nanotechnology.....	5
2.2 Nanoparticle.....	7
2.3 Gold nanoparticles.....	8
2.4 Cytotoxicity of gold nanoparticles.....	11
2.5 Mitochondria.....	17
CHAPTER III MATERIALS AND METHODS.....	21
3.1 Equipments.....	21
3.2 Chemicals and kits.....	22
3.3 Synthesis of citrate-stabilized gold nanoparticles.....	24
3.4 Characterization of gold nanoparticles.....	25
3.5 HeLa cell culture.....	25
3.6 Determination of cell morphology by light microscope.....	26
3.7 Determination of intracellular morphology and fate of gold nanoparticles by transmission electron microscope.....	26

	Page
3.8 <i>In vitro</i> cytotoxicity assay.....	27
3.9 RNA extraction.....	28
3.10 RT-PCR for mitochondrial gene expression in HeLa cell	
3.10.1 cDNA synthesis.....	29
3.10.2 PCR	
3.10.2.1 PCR for GAPDH expression.....	30
3.10.2.2 PCR for ATP synthase expression.....	30
3.10.2.3 PCR for Cyt b expression.....	30
3.10.2.4 PCR for CO1 expression.....	30
3.10.2.5 PCR for CO2 expression.....	31
3.10.2.6 PCR for ND3 expression.....	31
3.10.3 Agarose gel electrophoresis.....	31
CHAPTER IV RESULTS AND DISCUSSION.....	33
4.1 Characterization of gold nanoparticles.....	33
4.2 Effect of gold nanoparticles on cell morphology.....	35
4.3 <i>In vitro</i> cytotoxicity.....	42
4.4 Localization of gold nanoparticles.....	44
4.5 Mitochondrial gene expression	
4.5.1 GAPDH expression.....	48
4.5.2 ATP synthase expression.....	49
4.5.3 Cyt b expression.....	50
4.5.4 CO1 expression.....	51
4.5.5 CO2 expression.....	52
4.5.6 ND3 expression.....	53
CHAPTER V CONCLUSION.....	55
CHAPTER VI FUTURE PERSPECTIVE.....	56
REFERENCES.....	57

	Page
APPENDICES.....	61
APPENDIX A.....	62
APPENDIX B.....	64
BIOGRAPHY.....	66



ศูนย์วิทยทรัพยากร
จุฬาลงกรณ์มหาวิทยาลัย

LIST OF TABLES

Table	Page
1 The development and commercializing of nanomaterials.....	6
2 The cytotoxicity of gold nanoparticles.....	15
3 Primer sequences and PCR product sizes.....	32

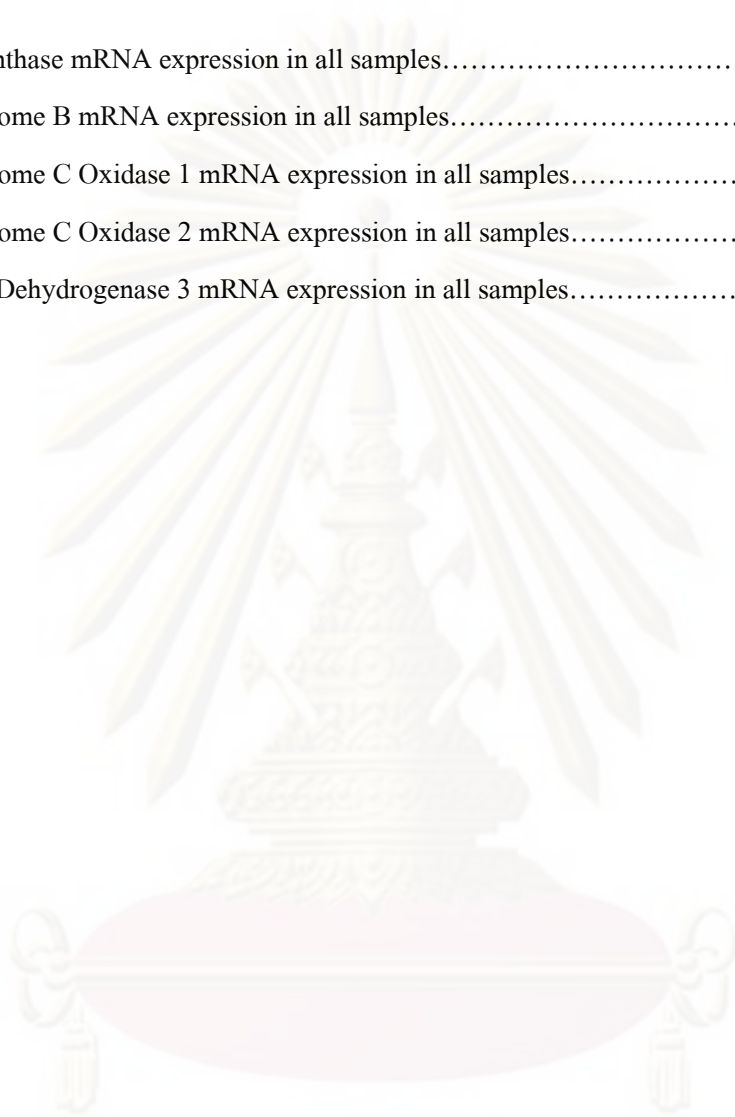


ศูนย์วิทยทรัพยากร
จุฬาลงกรณ์มหาวิทยาลัย

LIST OF FIGURES

Figure	Page
1 Mitochondrial genome and protein complexes.....	3
2 Optical properties of gold nanospheres and gold nanorods.....	7
3 Biomedical applications of gold nanoparticles.....	9
4 Basic principle of biosensors based on gold nanoparticles (protein detection).....	9
5 Basic principle of biosensors based on gold nanoparticles (DNA detection).....	10
6 Application of gold nanoparticles as contrast agent.....	11
7 Quantum dot labeling of the mitochondrial and microtubular network.....	19
8 Application of gold nanoparticles for probing mitochondrial membrane channels.....	20
9 Synthesis of gold nanoparticles by citrate reducing method.....	24
10 The morphology of HeLa cells.....	26
11 The characterization of gold nanoparticles using spectrophotometer.....	32
12 The characterization of gold nanoparticles using TEM.....	34
13 General cell morphology in negative control.....	36
14 HeLa cells morphology in positive control.....	37
15 HeLa cells morphology in the presence of citrate.....	38
16 HeLa cells morphology in the presence of 10 ug/mL AuNP.....	39
17 HeLa cells morphology in the presence of 50 ug/mL AuNP.....	40
18 HeLa cells morphology in the exposure to 100 ug/mL AuNP.....	41
19 The influence of gold nanoparticles on cell viability.....	43
20 Cellular uptake of 10-15 nm gold nanoparticles via the endocytosis.....	44
21 Internalization of gold nanoparticles.....	45
22 Intracellular organelles morphologyGAPDH mRNA expression in all samples.....	46
23 GAPDH mRNA expression in all samples.....	48

Figure	Page
24 ATP synthase mRNA expression in all samples.....	49
25 Cytochrome B mRNA expression in all samples.....	50
26 Cytochrome C Oxidase 1 mRNA expression in all samples.....	51
27 Cytochrome C Oxidase 2 mRNA expression in all samples.....	52
28 NADH Dehydrogenase 3 mRNA expression in all samples.....	53

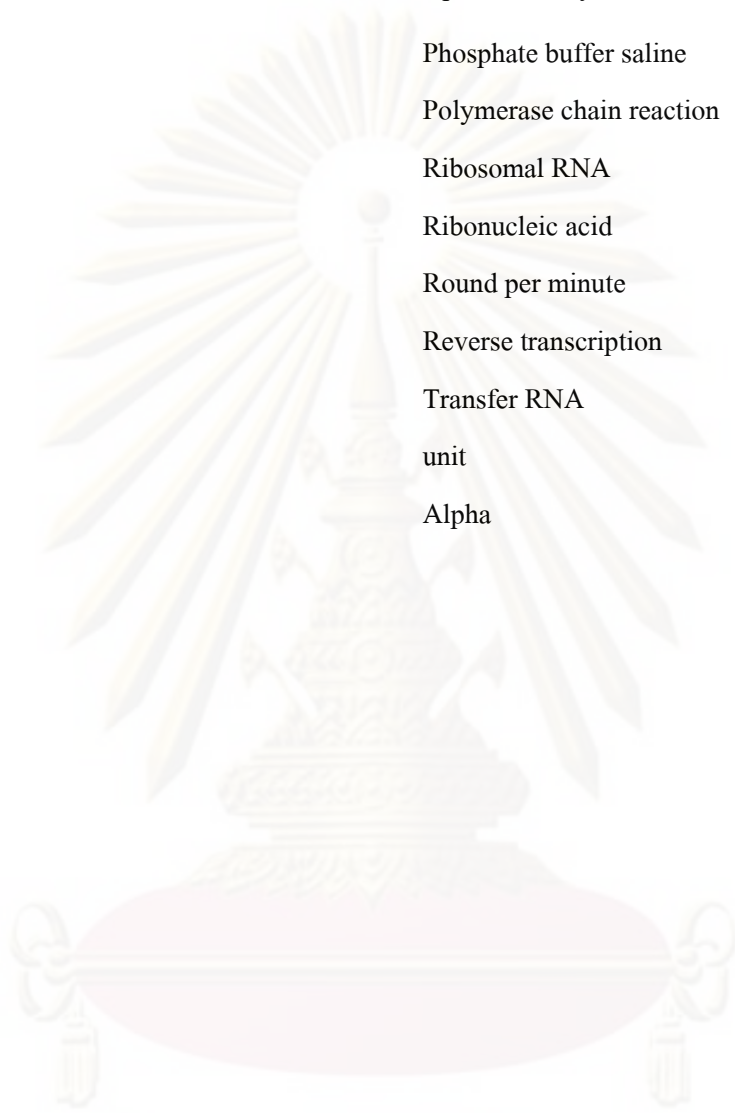


ศูนย์วิทยทรัพยากร
จุฬาลงกรณ์มหาวิทยาลัย

LIST OF ABBREVIATIONS

%	Percentage
°C	Degree Celsius
µg	Microgram
µL	Microliter
µm	Micrometer
µM	Micromolar
ATP	Adenosine triphosphate
AuNP	Gold nanoparticle
bp	Base pair
cDNA	Complementary DNA
Cyt b	Cytochrome B
CO1	Cytochrome C Oxidase 1
CO2	Cytochrome C Oxidase 2
DNA	Deoxyrironucleic acid
DMEM	Dulbecco's Modified Eagle's Medium
dNTP	Deoxynucleotide triphosphate
EDTA	Ethylene diamine tetraacetic acid
g (centrifugation speed)	Gravity
h.	Hour
M	Molar
mM	Millimolar
mg	Milligram
MgCl ₂	Magnesium Chloride
mL	Milliliter
mtDNA	Mitochondrial DNA
nM	Nanomolar

ND3	NADH Dehydrogenase 3
OD	Optical density
PBS	Phosphate buffer saline
PCR	Polymerase chain reaction
rRNA	Ribosomal RNA
RNA	Ribonucleic acid
rpm	Round per minute
RT	Reverse transcription
tRNA	Transfer RNA
u.	unit
α	Alpha



ศูนย์วิทยทรัพยากร
จุฬาลงกรณ์มหาวิทยาลัย

CHAPTER I

BACKGROUND

Nanotechnology is the ability to work at the atomic, molecular, and supramolecular levels (on a scale of ~1–100 nm) in order to understand, create, and use material structures, devices, and systems with fundamentally new properties and functions resulting from their small structure(1). Nanotechnology is a multidisciplinary field which comprises of the fundamental and applied sciences such as physics, chemistry, biology, medicine, and engineering.

Nanotechnology creates nanomaterials that are defined as materials produced within the range of 1-100 nm in length or diameter. Nanomaterials exhibit novel properties such as unique mechanical, optical, chemical, electrical and magnetic properties(2, 3). The unique properties of nanomaterials directly depend on their size and structure. Some widely-used nanomaterials available in public are nanoparticles, nanorods, nanowires, nanotubes, nanofilms, etc.

Among various type of nano gadgets, gold nanoparticles (AuNPs) particularly have been used in biomedical application, because the nanoparticulate sizes of gold exhibit astronomically high chemical reactivity(4, 5). The rich surface area of gold nanoparticle allows surface modification with wide varieties of biomolecules, for example: DNA(6-8), carbohydrate(9), drugs(10), and protein(11). Therefore, gold nanoparticles can be served as promising biotech tools such as biosensors, drug/gene delivery devices, and contrast agents.

Recently, prior study found the presence of AuNPs in mitochondria, an important energy producer of all eukaryotic cells. Salnikov *et al.* used gold nanoparticles to probe the mitochondria. By employing different sizes of gold nanoparticles to detect the permeability of the mitochondrial outer membrane, they found that 3 nm AuNPs were able to enter mitochondria, whereas the bigger sizes

could not access to the bilayers of mitochondrial membrane. Moreover, other biological aspects of subcellular organelles affected by AuNPs in the cells have not been clearly evaluated(12).

Although the applications and benefits of gold nanoparticles are extensive, the safety/toxicity profiles and nanotoxic studies of gold nanoparticles are limited. In particular, the effect of gold nanoparticles on gene expression, a cellular mechanism for RNA and protein synthesis, along with the cell viability, is not well clarified. Nevertheless, recent studies have demonstrated the cytotoxicity of gold nanoparticles in various cell lines. Thomas *et al.* reported that PEI-modified gold nanoparticles decreased COS-7 (kidney monkey cell lineage) viability to 70-80%(13). Tanya *et al.* reported that gold nanorod altered gene expression in HeLa cells such as *Fas* and *Ras*(14). In contrast, Connor *et al.* reported that different size gold nanoparticles that stabilized with any substances did not alter K562 (leukemic cell lineage) viability(15). Khan *et al.* reported that 18 nm citrate-stabilized gold nanoparticles were not toxic and changed gene expression in HeLa cells(16).

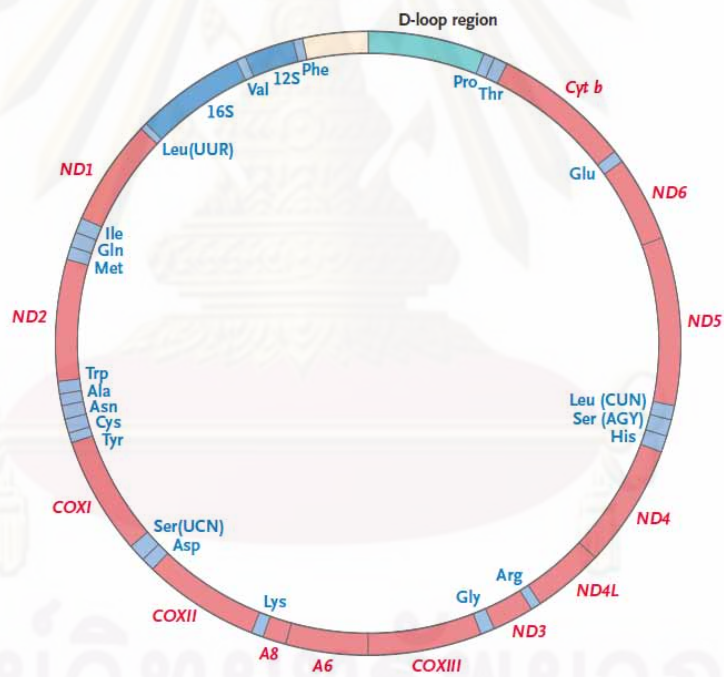
Mitochondria are important organelles due to its function to serve for cell survival. The prominent functions of the mitochondria are ATP generation, regulation of cellular metabolism and control of apoptosis process. Mitochondria have their own DNAs so they can independently synthesize their own specific RNA and functional proteins. Some of the important mitochondrial protein that are crucial for maintenance the cellular functions are ATP synthase, Cytochrome B, Cytochrome C Oxidase and NADH Dehydrogenase(17).

Despite gold nanoparticles are used in accessing, probing and manipulating mitochondria, there is a serious lack of information concerning the adverse effect of gold nanoparticles on mitochondria, especially the effect of gold nanoparticles on mitochondrial gene expression.

The purpose of this study is to investigate the influence of citrate stabilized-gold nanoparticles on cell viability and mitochondrial gene expression in mammalian cells. The mRNA expression of ATP synthase, Cytochrome B (Cyt. b), Cytochrome C Oxidase I (CO1), Cytochrome C Oxidase II (CO2) and NADH Dehydrogenase 3 (ND3) were selected as representative mitochondrial genes in

this work. These protein-coding genes play major roles in cellular control of various normal physiological processes, including cellular respiration, metabolic control and energy generation. In condition that there are changes of the transcription step of the delegate genes, the functional aberration would be taken place, leading to pathological stage of the affected cells. These genes were selected to symbolize mitochondrial protein complexes (complex 1, 3, 4 and 5) (17), as shown in figure 1. Additionally, the five chosen genes can be further divided into three groups according to their stability, reported by Piechota *et al.* The first group consists of CO1 and Cyt. b, which contains the most mRNA stability among the others. The second group, ND3 transcript, has the lowest stability. The third group, comprises of the CO2 and ATPase transcripts, have longer stability than first group(18).

A



ศูนย์วิทยุโทรพยากร
จุฬาลงกรณ์มหาวิทยาลัย

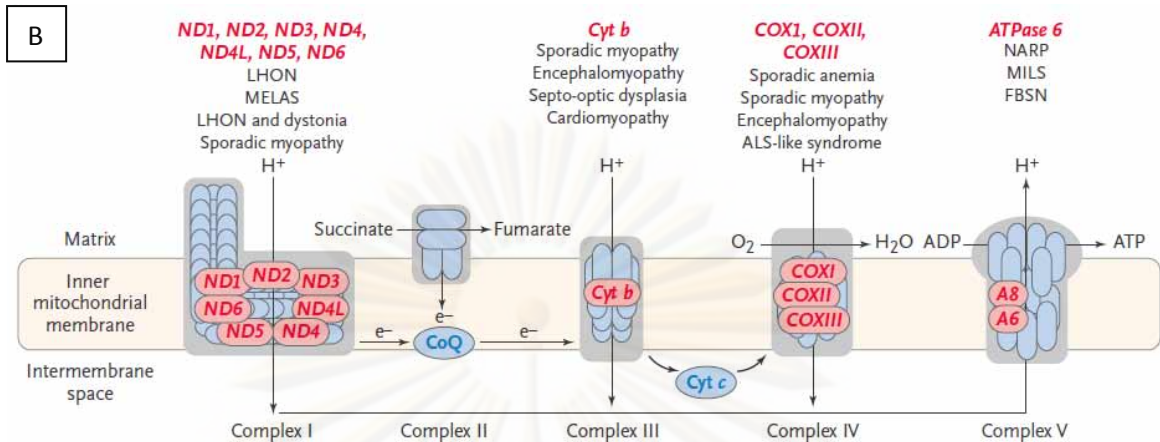


Figure 1 Mitochondrial genome and protein complexes. Fig 1A shows the map of the human mitochondrial genome. Fig 1B shows mitochondrial protein complexes at inner mitochondrial membrane.

In conclusion, this research work aims to explore some insight of the in vitro nano-bio interaction. The cell viability and gene expression are essential basic knowledge for determining the nanosafety/toxicity of any nanomaterial.

Objective

The propose of this research is to evaluate the influence of gold nanoparticles on mitochondrial gene expression in HeLa cells.

ศูนย์วิทยทรัพยากร
จุฬาลงกรณ์มหาวิทยาลัย

CHAPTER II

LITERATURE REVIEWS

2.1 Nanotechnology

Nanotechnology involves the creation and manipulation of materials at the nanoscale level to create unique products which have novel properties. Recently, nanomaterials such as nanotubes, nanowires, nanoparticles and quantum dots have received enormous attention in the creation of analytical tools for biotechnology and biomedical sciences. In biotechnology and biomedical sciences, there is a strong dependence on having proper understanding of biochemical processes, some of the nanomaterials developed including nanoparticles and quantum dots can be used to obtain much deeper understanding of biological processes(19).

Properties of the nanomaterials differ them from bulk materials because the nanomaterials have high surface-to-volume ratio and other size-dependent qualities. Additionally, some of different materials have been used to create nanomaterials such as carbon, semiconductor (quantum dots) and gold. Thus, the composition of these materials determines their biocompatibility and suitability for the relevant applications.

Nanotechnology is being applied to medical diagnostics and molecular diagnostics. The applications of nanomaterials to biology or medicine is given below: (20)

- Fluorescent biological labels(21)
- Drug and gene delivery(10, 13)
- Detection of proteins(22)
- Probing of DNA structure(23)

Nowadays, some of the companies that are involved in the development and commercialization of nanomaterials in biological and medical applications are listed below (see Table 1). Most of the companies are developing pharmaceutical applications, mainly for drug delivery. Several companies exploit quantum size effects in semiconductor nanocrystals for tagging biomolecules, or use bio-conjugated gold nanoparticles for labelling various cellular parts(20).

Company	Major area of activity	Technology
Advectus Life Sciences Inc.	Drug delivery	Polymeric nanoparticles engineered to carry anti-tumour drug across the blood-brain barrier
Alnis Biosciences, Inc.	Bio-pharmaceutical	Biodegradable polymeric nanoparticles for drug delivery
Argonide	Membrane filtration	Nanoporous ceramic materials for endotoxin filtration, orthopaedic and dental implants, DNA and protein separation
BASF	Toothpaste	Hydroxyapatite nanoparticles seems to improve dental surface
Biophan Technologies, Inc.	MRI shielding	Nanomagnetic/carbon composite materials to shield medical devices from RF fields
Capsulation NanoScience AG	Pharmaceutical coatings to improve solubility of drugs	Layer-by-layer poly-electrolyte coatings, 8–50 nm
Dynal Biotech		Magnetic beads
Eiffel Technologies	Drug delivery	Reducing size of the drug particles to 50–100 nm
EnviroSystems, Inc.	Surface disinfectant	Nanoemulsions
Evident Technologies	Luminescent biomarkers	Semiconductor quantum dots with amine or carboxyl groups on the surface, emission from 350 to 2500 nm
Immunicon	Tarcking and separation of different cell types	magnetic core surrounded by a polymeric layer coated with antibodies for capturing cells
KES Science and Technology, Inc.	AiroCide filters	Nano-TiO ₂ to destroy airborne pathogens
NanoBio Cortporation	Pharmaceutical	Antimicrobial nano-emulsions
NanoCarrier Co., Ltd	Drug delivery	Micellar nanoparticles for encapsulation of drugs, proteins, DNA
NanoPharm AG	Drug delivery	Polybutylcyanoacrylate nanoparticles are coated with drugs and then with surfactant, can go across the blood-brain barrier
Nanoplex Technologies, Inc	Nanobarcodes for bioanalysis	
Nanoprobes, Inc.	Gold nanoparticles for biological markers	Gold nanoparticles bio-conjugates for TEM and/or fluorescent microscopy
Nanoshpere, Inc.	Gold biomarkers	DNA barcode attached to each nanoprobe for identification purposes, PCR is used to amplify the signal; also catalytic silver deposition to amplify the signal using surface plasmon resonance
NanoMed Pharmaceutical, Inc.	Drug delivery	Nanoparticles for drug delivery
Oxonica Ltd	Sunscreens	Doped transparent nanoparticles to effectively absorb harmful UV and convert it into heat
PSiVida Ltd	Tissue engineering, implants, drugs and gene delivery, bio-filtration	Exploiting material properties of nanostructured porous silicone
Smith & Nephew	Acticoat bandages	Nanocrystal silver is highly toxic to pathogenes
QuantumDot Corporation	Luminescent biomarkers	Bioconjugated semiconductor quantum dots

Table 1 The development and commercialization of nanomaterials. Examples of companies commercializing nanomaterials for biological and medical applications.

2.2 Nanoparticle

A nanoparticle is, by definition, a particle with diameters ranging from 1 to 100 nm. Nanoparticles are known to exist in various shapes such as spherical, triangular, cubical, rod-shaped and shells. Nanoparticles have sizes similar to the biomolecules encountered at the cellular level. This unique size of nanoparticles facilitates the development of nanodevices that can be applied in medical and clinical applications. Moreover, nanoparticles contain different amount of atoms or molecules from their bulk materials. Therefore, nanoparticles exhibit electrical, optical and chemical properties that are very different from the bulk materials. For example, the prominent colors of metallic nanoparticle solutions such as gold nanoparticles are due to the red shift of the plasmon band to visible frequencies, unlike the bulk metals where the plasmon absorption is in the UV region. In fact, a plasmon is a quantum of collective oscillation of free electrons in the metals. Additionally, the optical properties of nanoparticles depend significantly on their size and shape as well as on the dielectric constant of the surrounding medium(24), as shown in figure 2.

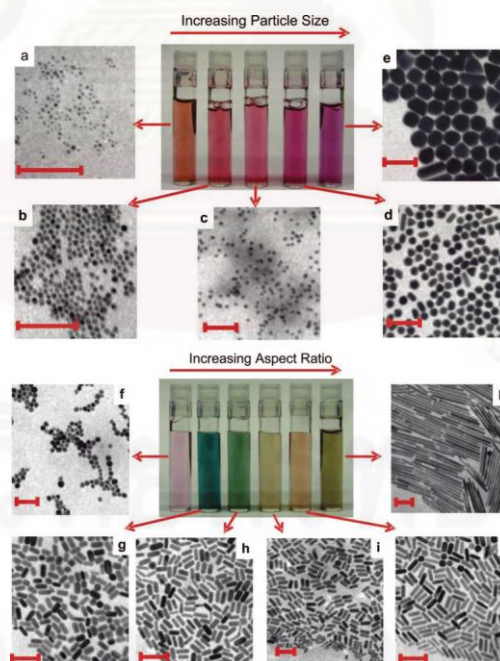


Figure 2 Optical properties of gold nanoparticles and nanorods. Photograph demonstrates the unique color of aqueous solutions of gold nanospheres (upper panels) and gold nanorods (lower panels).

2.3 Gold Nanoparticle (AuNP)

Gold is very popular for being chemically inert metals. It is indeed one of the most stable metals in the group eight elements, and it resists to oxidation(25) An aqueous gold solution is synthesized to be colloidal gold nanoparticles which have an average size at 1-100 nm with unique properties. Due to the simplicity and high yield, the most commonly used method for preparation of gold nanoparticles is the citrate reduction method of Turkevich *et al*(26). In 1951, Turkevitch *et al.* reported the formation of gold nanoparticles by the reduction of an aqueous solution of hydrogen tetrachloroaurate (HAuCl_4) using citrate in water. The utilization of citrate as a capping agent is very convenient to post-synthesis treatment, since it can be easily replaced by other capping agents such as thiol. Thiol is an appropriate capping agent for binding of the biological analyte(26).

The nanoparticulate sizes of gold display unique physical and chemical properties. Furthermore, the rich surface area of gold nanoparticles allows surface modification with varieties of ligands. The surface related properties are affected with modification of size, shape and surrounding media of gold nanoparticles. Therefore, the desired optical properties of gold nanoparticles can be tuned by generating the distinct size and shape of gold nanoparticles in desired media.

Gold nanoparticles solution is normally bright red color with the plasmon absorption band centered at 520 nm. But any surface modification of gold nanoparticles results in the shift of plasmon absorption wavelength. This change in optical property of gold nanoparticles is exploited to develop biosensors(27). Additionally, surface plasmon resonance is an optical technique that measuring the refractive index of very thin layers of material adsorbed on a metal. Plasmon resonance is a result from the binding of gold nanoparticles-labels and specific targets. This interaction leads to changes in optical properties that can be used for biomolecular detection. It is known that the characteristic red color of gold nanoparticles changes to a bluish-purple color on colloidal aggregation because of the plasmon resonance(28).

As mentioned above, gold nanoparticles have been widely used in biomedical applications including tracking, sensing, drugs/genes delivery devices and imaging, as shown in figure 3.

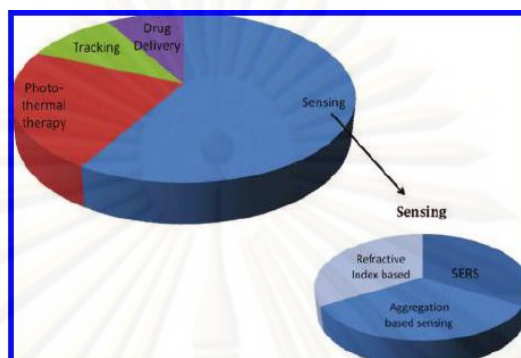


Figure 3 Biomedical applications of gold nanoparticles. Gold nanoparticles are used as biosensors, photothermal therapy and drug delivery.

Gold nanoparticles provide great sensitivity for the detection of DNA and proteins(29). They can be labeled with DNA or protein molecules (including antigens and antibodies), which can bind to their targets. This basic principle involved in the design of the biosensors based on gold nanoparticles. Gold nanoparticles are functionalized or capped with a thiolated biomolecule which detecting the targeted biomolecule and resulting change in the optical absorption of gold nanoparticles(30).

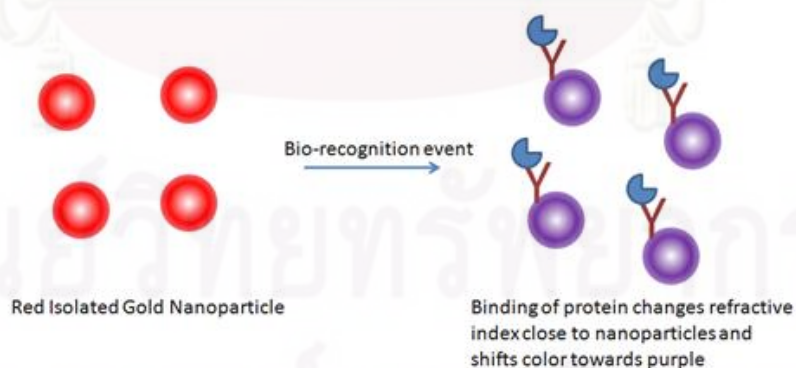


Figure 4 Basic principle of biosensors based on gold nanoparticles (protein detection).

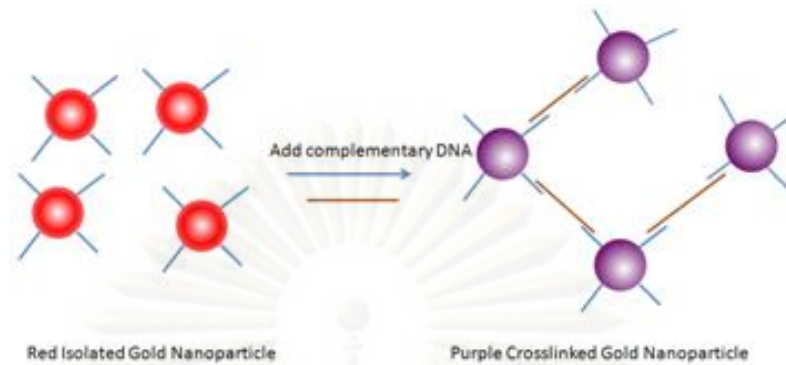


Figure 5 Basic principle of biosensors based on gold nanoparticles (DNA detection).

The biosensors based on gold nanoparticles along with immunoassays have been developed. The immunoassays are the antigen-antibody interactions. Gold nanoparticles functionalized with antigen or antibody aggregate when binding antibody or antigen and cause a shift in the plasmon absorption. For example, aptamer functionalized gold nanoparticles specifically binds to thrombin resulting in aggregation of gold nanoparticles and red shifting the plasmon absorption. The specific binding was tested by exposing aptamer functionalized gold nanoparticles to other proteins (BSA or human IgG antibodies) where gold nanoparticles aggregation was not observed(22).

In 2006, Hainfeld *et al.* have demonstrated the utilization of gold nanoparticles as X-ray contrast agents in imaging breast cancer. The 1.9 nm gold nanoparticles were injected via a tail vein into Balb/C mice bearing EMT-6 subcutaneous mammary tumors. Gold nanoparticles can be used as X-ray contrast agents with properties that overcome some significant limitations of iodine-based agents(21).

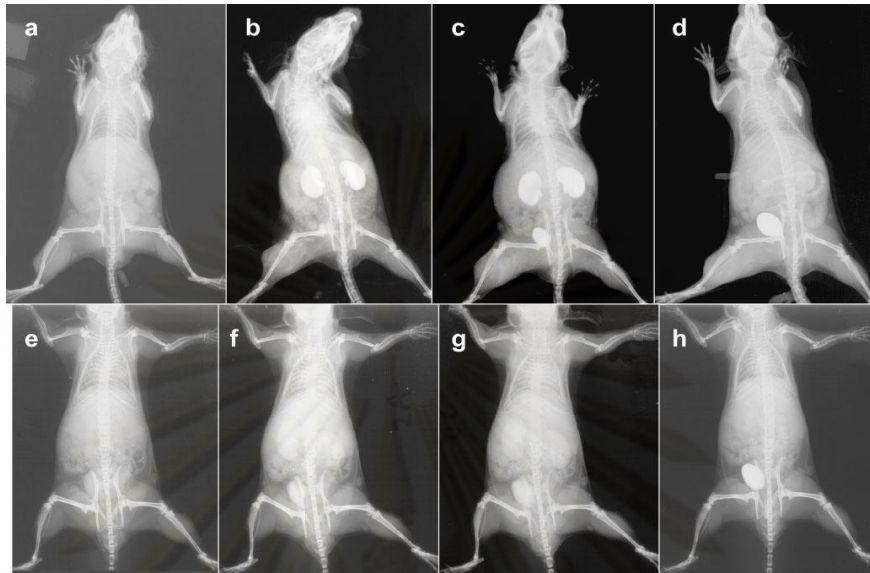


Figure 6 Application of gold nanoparticles as contrast agent. Pharmacokinetics of gold nanoparticles (a–d) and iodine contrast agent (e–h) in mice. (a,e) Before injection. (b,f) 2 min after injection; (c,g) 10 min after injection; (d,h) 60 min after injection. Gold nanoparticles show low liver and spleen uptake and clearance via kidneys and bladder (b–d). At 60 min (d), the contrast in the gold-injected mouse is similar to the uninjected mouse (a), indicating efficient clearance.

Thomas *et al.* have functionalized gold nanoparticles with branched 2 kDa polyethylenimine (PEI) to create transfection vectors. It was found that the transfection efficiency into monkey kidney (Cos-7) cells varied with the PEI/gold molar ratio in the conjugates. The results indicated that increasing the hydrophobicity of the transfection agent enhances cellular internalization(13).

2.4 Cytotoxicity of gold nanoparticles

Many studies have suggested that gold nanoparticles are biocompatible and can be used safely. This thought may be due to the established safety of bulk gold, but the nanoparticulated gold will behave very differently than in bulk gold(31). Because of their small size, gold nanoparticles have

been found to easily enter cells. Thus, several groups have examined the cellular uptake and cytotoxicity of gold nanoparticles.

Early studies with cytotoxicity data were focused on utilizing this property for nuclear transfection and targeting. The purpose of their work was to find nonviral gene-delivery devices, Thomas *et al.* reported polyethylenimine (PEI)-modified gold nanoparticles could transfect monkey kidney (COS-7) cells six times better than PEI alone. The cell viability was tested after exposure to PEI-gold nanoparticle complexes, and 80% of the cells were still metabolically active. While PEI-gold nanoparticles with dodecyl-PEI complexes achieved even better transfection, and cell viability was decreased to 70%. This complex was mainly found inside the cell suggesting that internalization is a factor in cytotoxicity. However, as the gold nanoparticles were conjugated to PEI, whether or not the observed decrease in cell viability was due to the gold nanoparticles is unclear(13).

In 2003, Tkachenko *et al.*, looked first at the nuclear targeting ability of gold nanoparticles alone, and then at gold nanoparticles with a full-length peptide containing both the receptor-mediated endocytosis and nuclear localization signal segments from an adenovirus in HepG2 cells. They found that naked gold nanoparticles were readily taken up into the cytoplasm but they did not enter the nucleus. Other experiments conducted at 4°C indicated that cell entry was energy dependent since a decrease in the number of particles inside the cells was observed. However, the nanoparticle-peptide complex incorporating both transport signals was found to enter the nucleus. Despite this nuclear exposure, cell viability was greater than 95% after 12 hours of incubation(32).

Moreover, Tkachenko *et al.* conducted another study examining four different peptide-BSA-gold nanoparticle conjugates in three cell lines (HeLa, 3T3/NIH, and HepG2). They reported different effects of gold nanoparticles between the three cell lines. The four peptide-BSA-gold nanoparticles were able to enter and escape the endosomes in HeLa cells. But gold nanoparticles with the HIV Tat protein were able to enter the nucleus in HeLa cells. In contrast, the four peptide-BSA-gold nanoparticles were found clustered together in endosomes within the 3T3/NIH cells. The HepG2 cells did not seem to uptake the peptide-BSA-gold nanoparticles except for the gold nanoparticles with the

integrin-binding domain. The LDH cytotoxicity assay also confirmed these cell-line differences. After three hours of incubation, the peptide-BSA-gold nanoparticles conjugated with the adenovirus protein caused 20% cell death in HeLa cells while only 5% in the 3T3/NIH cells. This suggests that the nuclear delivery of the peptide-BSA-gold nanoparticles influences cell viability due to particle interactions with cellular DNA(33).

Goodman *et al.* also tested the effect of 2 nm gold nanoparticle functionalized with both cationic and anionic surface groups in multiple cell lines. Cationic (ammonium-functionalized) and anionic (carboxylate-functionalized) gold nanoparticles with concentrations of 0.38–3 μM were incubated with COS-1 cells, red blood cells, and *Escherichia coli* cultures for 24 hours. While the cationic gold nanoparticles were clearly more cytotoxic than the anionic gold nanoparticles. Furthermore, a small variation was observed in their LC50 values between cell types, showing that the different cell types exhibit similar toxicity(34).

Pernodet *et al.* were examined the influence of 13 nm citrate-capped gold nanoparticles on cell proliferation, morphological structure, spreading, migration, and protein synthesis of human dermal fibroblast cells. They found that cell area decreased along with cell number and density of actin fibers depend on the increasing concentration of gold nanoparticles. The number of vacuoles present within the cells increased upon the increasing incubation time. The decreased number of cells indicates some cytotoxic effects. They concluded that 13 nm citrate-capped gold nanoparticles were toxic by promote the formation of abnormal actin filaments and lead to decrease in cell proliferation, adhesion, and motility. Moreover, the observed cellular changes were both dose and time-dependent patterns(35).

Cytotoxicity may not be the only adverse effect of gold nanoparticles on cellular changes but gold nanoparticles may also affect the immunological response of cells. Shukla *et al.* tested the effect of gold nanoparticles on the proliferation, nitric oxide, and reactive oxygen species production of RAW264.7 macrophage cells. After 48 hours of up to 100 μM gold nanoparticle treatment, RAW264.7 macrophage cells showed greater than 90% viability with no increase in pro-inflammatory

cytokines TNF- α and IL-1 β . Cell viability decreased to 85% after 72 hours, which was attributed to depletion of media nutrients since the media was not changed in those 72 hours. They found that cells take up gold nanoparticles in lysosomes, which move in a time-dependent pattern toward the nucleus but do not enter the nucleus(36).

Furthermore, other non-cytotoxic effects of gold nanoparticles have been found. Connor *et al.* studied the effect of size and different surface modifications on uptake and acute toxicity in human leukemia (K562) cells. The sizes ranged between 4 and 18 nm with surface modifiers including biotin, CTAB, cysteine, citrate, and glucose. The K562 leukemia cell line was exposed to the nanoparticles for three days then, cell viability was determined using a colorimetric MTT assay. After three days of exposure, the largest nanoparticle with citrate and biotin surface modifiers did not appear to be toxic at concentrations up to 250 μ M. They reported that gold nanoparticles are non-toxic to human cells despite being taken up into the cells. However some precursors used to generate gold nanoparticles might be toxic. Thus, the toxicity of gold nanoparticles can be controlled by using non-toxic reagents to produce them(15).

Recently Hauck *et al.* have reported that gold nanorods coated with CTAB showed 90% cell viability for HeLa cells and caused little changes in level of gene expression (only 35 from 10,000 genes) examined were mildly down-regulated(14).

In 2007, Khan *et al.* determined for the transcriptional profile of HeLa cells in the presence of 18 nm citrate-capped gold nanoparticles. They generated transcriptional profiles of HeLa cells incubated with 18 nm gold nanoparticles for 6 h. The results showed that the expression level of most of the genes remained unaltered(16). The results from Hauck *et al.* are similar to Khan *et al.* which demonstrated that gold nanoparticles did not alter level of gene expression.

A summary of the experimental setup and results on gold nanoparticles is provided in Table 2(37).

Author	Cell line	Surface coating	NP concentration	Average size (nm)	Test	Exposure duration	Toxicity
Shukla	RAW264.7 mouse macrophage cells	lysine,poly (L-lysine)	10, 25, 50, and 100 uM	3.5± 0.7	MTT	24, 48, 72 h	Cell viability decreased to 85% after being exposed to 100 uM AuNP for 72 h.
Connor	K562 human leukemia	citrate, cysteine, glucose, biotin, CTAB	0-250 uM	4,12, 18	MTT	3 days	No apparent toxicity at 250 uM, glucose and cysteine modified not toxic up to 25 uM
Goodman	COS-1 cells, Red blood cells, E. coli	Quaternary ammonium, carboxylic acid	0.38, 0.75, 1.5, or 3 uM	2	MTT, Trypan blue	1, 2.5, 6, 24 h	Cationic nanoparticles were found to be much more toxic than anionic particles of the same size. LD50 (Cos-1): anionic ~1 uM and cationic >7.37 uM; similar for other cell types.

Table 2 The cytotoxicity of gold nanoparticles.

Author	Cell line	Surface coating	NP concentration	Average size (nm)	Test	Exposure duration	Toxicity
Khan	HeLa cells	citrate	0.2-2 nM	18	MTT	3, 6 h	- AuNPs did not cause significant gene-expression patterns or cytotoxicity even though they were internalized in the cells.
Thomas	COS-7 cells	PEI	-		MTT	6, 42 h	70-80% viability after transfection
Tkachenko	Human liver carcinoma, HepG2	BSA, targeting peptides	-	20-25	LDH	12 h	Viability slightly compromised (<5%)
Tkachenko	HeLa, 3T3/NIH, HepG2	BSA, targeting peptides	150 pM	22	LDH	3 h	Cell viability reduced by 20% in HeLa cells, but only 5% in 3T3/NIH
Pernodet	Human dermal fibroblasts	citrate	0-0.8 mg/mL	12-14	Microscopy	2-6 days	Dose-dependent decrease in cell area & density; many vacuoles

Table 2 The cytotoxicity of gold nanoparticles.

ศูนย์วิทยาศาสตร์สุขภาพ
จุฬาลงกรณ์มหาวิทยาลัย

2.5 Mitochondria

Mitochondrion is the power house of the cell which is essential for the generation of energy (adenosine triphosphate, ATP). This organelle is crucial in the regulation of programmed cell death (apoptosis). Furthermore, mitochondria are critically involved in modulating the intracellular calcium concentration. The mitochondria play a crucial role in numerous catabolic and anabolic cellular pathways. Structurally, mitochondria have four compartments which comprise of the outer membrane, the inner membrane, the intermembrane space, and the matrix (the region inside the inner membrane)(17).

Mitochondria are the only organelles of the cell besides the nucleus that contain their own DNA and their own materials for RNA and proteins synthesis. The human mitochondrial DNA (mtDNA) is a 16,569 bp, double-stranded, circular molecule containing 37 genes (Figure. 1A). Of these, 24 are needed for mtDNA translation (2 ribosomal RNAs [rRNAs] and 22 transfer RNAs [tRNAs]), and 13 encode subunits of the respiratory chain which consist of seven subunits of complex I (ND1, 2, 3, 4, 4L, 5, and 6 [ND stands for NADH dehydrogenase]), one subunit of complex III (cytochrome *b*), three subunits of cytochrome *c* oxidase (COX I, II, and III), and two subunits of ATP synthase (A6 and A8). The inner mitochondrial membrane consists of five protein complexes(17) (Figure. 1B).

ศูนย์วิทยทรัพยากร
จุฬาลงกรณ์มหาวิทยาลัย

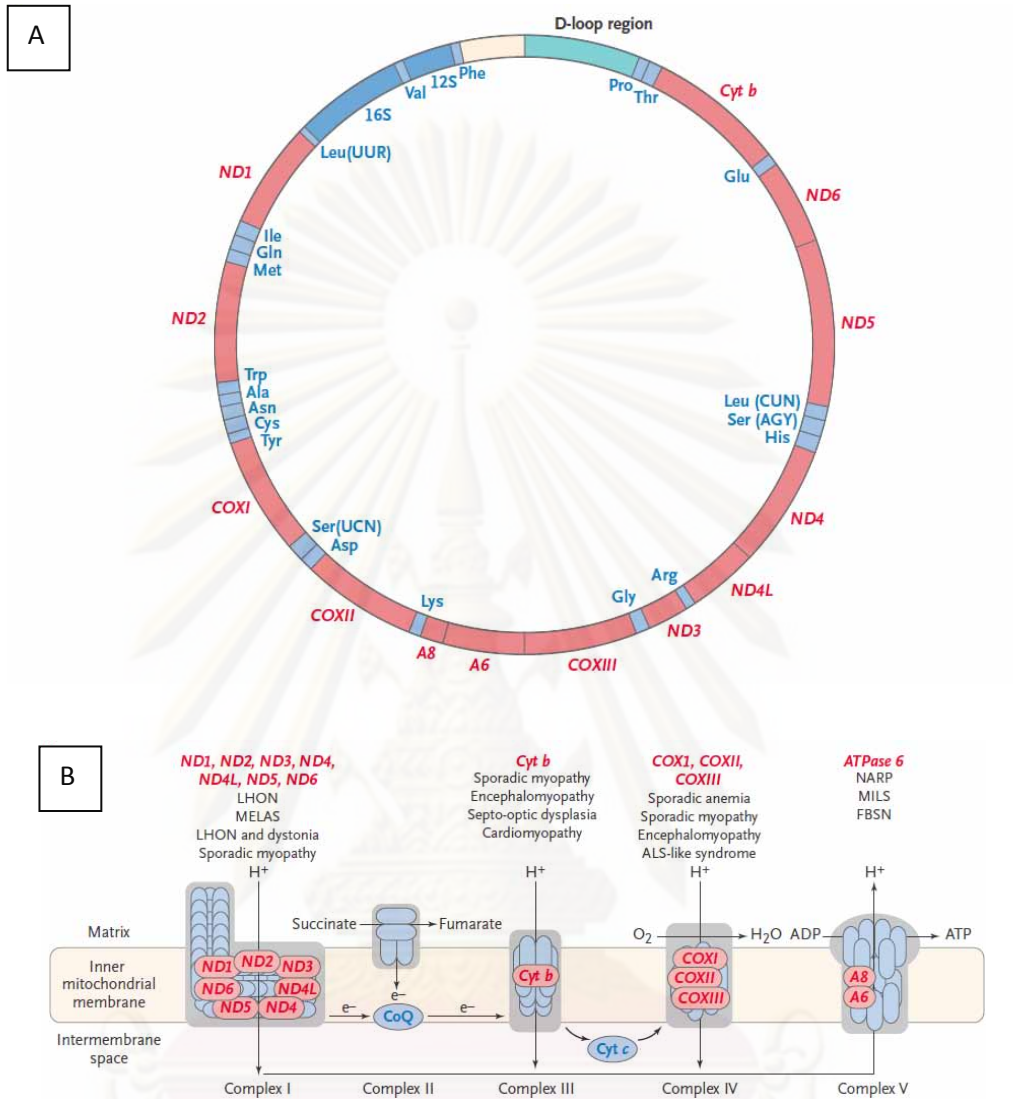


Figure 1 Mitochondrial genome and protein complexes. Fig 1A shows the map of the human mitochondrial genome. Fig 1B shows mitochondrial protein complexes at inner mitochondrial membrane.

The following example of how nanotechnology is capable of providing the well-needed tools for probing and manipulating mitochondria:

Medda *et al.* were able to provide insight into the association and interaction between mitochondria and cytosolic microtubules. They used the advantages of quantum dot staining over the conventional fluorophores. The results were observed using two-color 4Pi microscopy. They incubated

triton-permeabilized cells with anti- α -tubulin rabbit immunoglobulin G and anti- α -subunit of F_1F_0 -ATP-synthase mouse immunoglobulin G, followed by an addition of corresponding secondary antibodies conjugated to QDot® 605 and QDot® 655, respectively. The results demonstrated that the green microtubule was intertwined with the red mitochondria(38), as shown in figure 7.

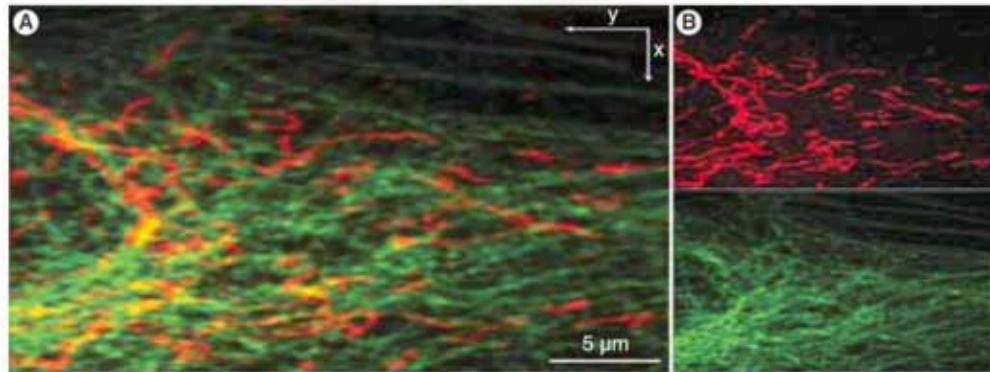


Figure 7 Quantum dot labeling of the mitochondrial and microtubular network.

Salnikov *et al.* employed different sizes of gold nanoparticles (AuNPs) to probe the permeability of the mitochondrial outer membrane. They were able to assess the physical diameter of the VDAC most likely to be between 3 and 6 nm. The investigators incubated rat permeabilised ventricular cells as well as isolated mitochondria under different conditions with 3 nm and 6 nm AuNPs, respectively. They found that while the outer mitochondrial membrane was impermeable to 6 nm AuNP in the absence of permeability transition, the smaller 3 nm AuNPs were able to enter mitochondria even in the presence of Cyclosporin A, which is known to prevent mitochondrial permeability transition(12), as shown in figure 8.

ศูนย์วิทยทรัพยากร
จุฬาลงกรณ์มหาวิทยาลัย

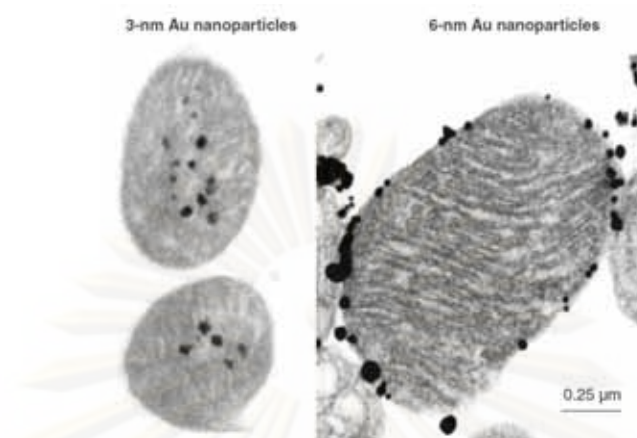


Figure 8 Application of gold nanoparticles for probing mitochondrial membrane channels.

In conclusion, the effect on gold nanoparticles on mitochondrial gene expression was not clearly understood. Thus, this study citrate-stabilized gold nanoparticle have been generated, characterized and tested for *in vitro* cytotoxicity including cell viability, cell morphology and intracellular localization especially, mitochondrial gene expression in HeLa cells in the presence of gold nanoparticles.

CHAPTER III

MATERIALS AND METHODS

3.1 Equipments

1. -80°C Deep Freezer model MDF-U32V Sanyo, Japan
2. -20°C Freezer Sanyo, Japan
3. 4°C Refrigerator Sanyo, Japan
4. 24 well plate Costar, USA
5. Autoclave Hirayama, Japan
6. Cell culture plates 25 and 75 cm \square Corning, USA
7. Cell scraper Greiner bio-one, Germany
8. Centrifuge Beckman Coulter, USA
9. Centrifuge Sorvall, Germany
10. Cuvette Hellma, Germany
11. Disposable pipette 1, 2, 10 and 20 mL Costar, USA
12. DNA Thermal Cycle Biometra, Germany
13. Gel Document and Quantity One 4.4.1 Biorad, USA
14. Gel Mate 2000 Electrophoresis Toyobo, Japan
15. Heat Block : Dri-Bath Type 17600 Thermolyne, USA
16. Heat Block : Thermo Block TDB-120 Biosan, USA
17. Hot Air Oven Shel Lab, USA
18. Incubator Precell (Jencous-PLS), USA
19. Lamina Flow Bioquell, UK
20. Light Microscope Nikon, Japan
21. Magnetic Stirrer Clifton, USA

22. Microcentrifuge : Minispin	Eppendorf, Germany
23. Microcentrifuge Tube 0.5 mL and 1.5 mL	Axygen Scientific, USA
24. Micropipette P2.5, P10, P100 and P1000	Biohit, Finland
25. Microwave	Imarflex, Thailand
26. PCR Tube 200 μ L	Axygen Scientific, USA
27. Power Supply	Hoffer Scientific Instrument, USA
28. Spectrophotometer	Biorad, USA
29. Stirrer Hot Plate	BEC Thai, Thailand
30. Transmission Electron Microscope	Jeol, USA
31. Tube 15 mL and 50 mL	Corning, USA
32. UV-Visible Spectrophotometer	BioMate, USA
33. Vortex Mixer	Gemmy Industrial, Taiwan
34. Water Bath	Thelco, USA

3.2 Chemicals and kits

1. 100 bp DNA Ladder	Fermentas, Canada
2. 100 mM dNTP Mix	Fermentas, Canada
3. 6X Loading Dye Solution	Fermentas, Canada
4. Absolute Ethanol	Bio Basic Inc., Canada
5. Agarose Gel	Research Organics Inc., USA
6. Antibiotic	Invitrogen, USA
7. DEPC (diethylpyrocarbonate)	Sigma Aldrich, USA
8. DMSO (Dimethyl sulfoxide)	Bio Basic Inc., Canada
9. DNase I	Fermentas, Canada
10. DMEM (Dulbecco's Modified Eagle's Medium)	Sigma Aldrich, USA
11. EDTA (ethylenediaminetetraacetic acid)	Fermentas, Canada
12. Ethidium Bromide	Sigma Aldrich, USA

13. Fetal bovine serum	Invitrogen, USA
14. Glacial acetic acid	Merck, Germany
15. Hydrogen tetracholoaurate (III) trihydrate	Sigma Aldrich, USA
16. Isopropanol	Bio Basic Inc., Canada
17. M-MuLV Reverse Trancriptase	Fermentas, Canada
18. Magnesium Chloride (MgCl ₂)	Fermentas, Canada
19. MTT	USB, USA
20. Phase separation Reagent : BCP	MRC, UK
21. Potassium chloride	Merk, Germany
22. Potassium phosphate	Merk, Germany
23. Ransom Hexamer Primer	Fermentas, Canada
24. Ribolock™ Ribonuclease Inhibitor	Fermentas, Canada
25. RNase, DNase Free Water	Invitrogen, USA
26. Sodium Carbonate	Merk, Germany
27. Sodium chloride	Merk, Germany
28. Sodium phosphate	Merk, Germany
29. Taq DNA Polymerase	Fermentas, Canada
30. Tris base	Research Organics Inc., USA
31. Trisodium citrate dihydrate	Merk, Germany
32. Trizol Reagent	Invitrogen, USA
33. Trypsin	Invitrogen, USA

ศูนย์วิทยทรัพยากร
จุฬาลงกรณ์มหาวิทยาลัย

3.3 Synthesis of citrate-stabilized gold nanoparticles (citrate-stabilized AuNPs)

Citrate reduction method was first proposed by Turkevich *et al.* in 1951(26). In a typical standard citrate reduction procedure, 45 mL of deionized water was heated to 90-100 °C on a stirrer hot plate under refluxing condition. While stirring vigorously, 2 mL of 1% hydrogen tetrachloroaurate (HAuCl_4) and 3.76 mL of 38.8 mM trisodium citrate ($\text{Na}_3\text{Citrate}$), a reducing agent were quickly added, resulting in color changes of the originally yellow solution to transparent. Then, the solution immediately turned to grey and purple, respectively. This solution was allowed to continue stirring for 2 hours. Finally, the observation of a deep red color indicates the formation of gold nanoparticles. The solution of gold nanoparticles was kept at 100 °C for 15 minutes and subsequently cooled to room temperature. The final gold nanoparticles are approximately spherical and have a negatively charged surface. The concentration of the synthesized gold nanoparticles is 200 $\mu\text{g/mL}$. See figure 9 for synthesis method of gold nanoparticles.

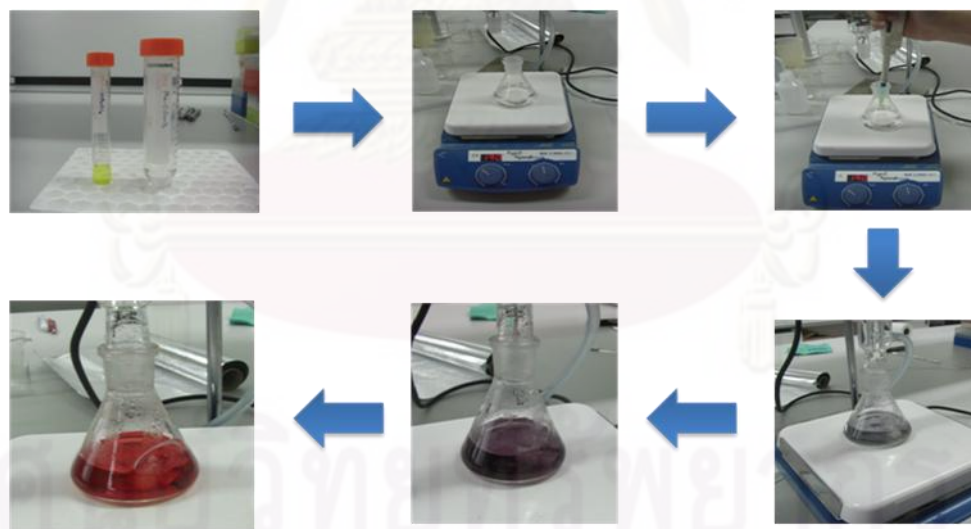


Figure 9 Synthesis of gold nanoparticles by citrate reducing method.

3.4 Characterization of gold nanoparticles

The synthesized AuNPs are commonly characterized by absorption spectroscopy and Transmission Electron Microscopy (TEM). The optical property, size and size distribution of gold nanoparticles were investigated and demonstrated as the plasmon wavelength (λ_{\max}) and plasmon width ($\Delta\lambda$). The plasmon wavelength (λ_{\max}) indicates size of gold nanoparticles and plasmon width ($\Delta\lambda$) indicates size distribution of gold nanoparticles. 1 mL of gold nanoparticle solution was pipetted in disposable cuvette and measured the absorption using UV-Vis Spectrophotometer.

A Transmission Electron Microscope (TEM) was used to view and determine the size and size distribution of gold nanoparticles. TEM samples were prepared as follows: a single drop (10 μ L) of gold nanoparticles solution was placed onto a copper grid. The grid was left to dry for several hours at room temperature. Then, the average size and size distribution histogram of AuNPs were determined by digital processing of Transmission Electron Microscopy images.

3.5 HeLa cell culture

This study used HeLa cell lines (cervical cancer cells) which were kindly provided by Prof. Dr. Apiwat Mutirangura. See figure 10 for the morphology of HeLa cells. HeLa cell lines were maintained in DMEM medium, supplemented with 10% fetal bovine serum and 1% antibiotics. Cells were incubated at 37 °C with 5% CO₂ atmosphere. The cells were subcultured and fed as needed. For the experiment, cells were seeded in 24 well plate at a density of 1×10^5 cells per well in 500 μ L of complete medium, triplicate samples. The cells were incubated for 24 hours at 37 °C with 5 % CO₂. After 24 hours incubation, the cells were added with DMSO as positive control and various concentrations gold nanoparticles (10, 50, and 100 μ g/mL respectively). After that, cells were further incubated for 1, 2, and 3 days at 37 °C with 5 % CO₂.

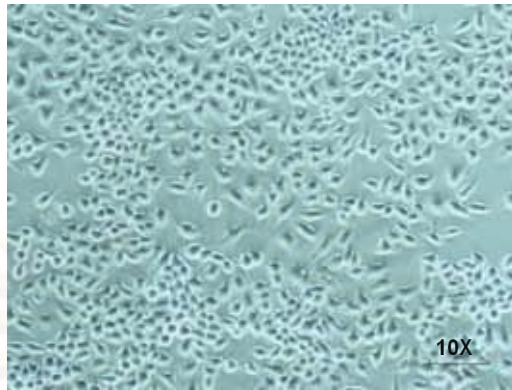


Figure 10 The morphology of HeLa cells.

3.6 Determination of cell morphology by Light Microscope (LM)

The effect of gold nanoparticles on cell morphology was determined using light microscope. After incubation cells with gold nanoparticles, cells were monitored and taken the picture by light microscope. The morphology of gold nanoparticles treated groups was compared with negative and positive control.

3.7 Determination of intracellular morphology and fate of gold nanoparticles by Transmission Electron Microscope (TEM)

The effect of gold nanoparticles on intracellular morphology as well as gold nanoparticles trafficking was determined using Transmission Electron Microscope (TEM). Cells were prepared as follows: after incubation with gold nanoparticles, cells were trypsinized and washed with PBS 2 times (10 minutes), followed by centrifugation at 2000 rpm for 5 minutes. The precipitate was prefixed in 2% glutaraldehyde for 2 hours and washed with PBS 3 times (10 minutes). Then, the precipitate was postfixed in 2% osmium tetroxide for 1 hour, centrifuged at 14000 rpm for 5 minutes and washed

with PBS 1 time (10 minutes). After that, the precipitate was dehydrated in ethanol series (50%, 70%, 80%, 95%-2 times and 100%-3 times, respectively). The precipitate was infiltrated in 100% propylene oxide for 2 hours, propylene oxide: epoxy resin (1: 1) for 3 hours and 100% epoxy resin for 18 hours. Finally, the precipitate was embedded in epoxy resin at 60°C overnight. Epoxy resin blocks were cut as ultra thin section (~ 60-90 nm), laid on the grid and stained with uranyl acetate and lead citrate. Samples were taken to monitor and take pictures by transmission electron microscope. The intracellular morphology of gold nanoparticles treated groups were compared with control groups.

3.8 *In vitro* Cytotoxicity assay (MTT)

In vitro Cytotoxicity was determined by MTT assay (3-(4,5-dimethylthiazol-2-yl)-2,5-diphenyl tetrazolium bromide). MTT assay is a colorimetric assay according to a tetrazolium-based compound is reduced to formazan by mitochondrial dehydrogenase in the living cells. Whereas, dead cells can not reduce tetrazolium-based compound to formazan because of lacking of mitochondrial dehydrogenase. The amount of formazan is directly proportional to the number of living cells in the culture. Formazan was measured with a spectrophotometer at 570 nm.

For the experiment, cells were seeded in 24 well plate at a density of 1×10^5 cells per well in 500 μ l of complete medium, triplicate samples. The cells were incubated for 24 hours at 37 °C with 5 % CO₂. After 24 hours incubation, cells were exposed to various concentrations of gold nanoparticles. Then, cells were further incubated for 1, 2 and 3 days. After 1, 2 and 3 days incubation, cells were washed with PBS 2 times, followed by added 350 μ L of the tetrazolium-based compound to each well. Cells were incubated in the incubator for 30 minutes. Cells were removed the tetrazolium-based compound and dissolved formazan with 1 ml of DMSO: glycine buffer (9: 1). The formazan solution was pipetted into cuvettes and measured optical density by spectrophotometer at 570 nm. The relative cell viability (%) relates to control wells containing cell culture without gold nanoparticles was calculated by using the following equation.

$$[A]_{\text{test}} / [A]_{\text{control}} \times 100$$

Where $[A]_{\text{test}}$ is the absorbance of the test sample and $[A]_{\text{control}}$ is the absorbance of control sample(39).

3.9 RNA extraction

After 1, 2 and 3 days incubation with gold nanoparticles, cells were trypsinized and washed with PBS 2 times, followed by centrifugation at 150 g for 5 minutes and the supernatant was removed. RNA was extracted by TRIzol reagent according to the manufacturer's instruction as follows: 10^5 - 10^6 cells were homogenized in 1 ml of TRIzol reagent and incubated for 5 minutes at room temperature. 200 μ L of BCP (phase separation reagent) was added and incubated for 3 minutes at room temperature before centrifugation at 12,000 g for 15 minutes at 4°C. Then, the aqueous phase was transferred to a new centrifuge tube. The RNA was precipitated by mixing with 0.5 ml of isopropyl alcohol. Samples were incubated for 10 minutes at room temperature, and followed by centrifuged at 12,000 g for 10 minutes at 4°C. The supernatant was removed and the RNA pellet was washed with 1 ml of 75% ethanol. Finally, 21 μ L of RNase/DNase-free water was added to dissolve the RNA pellet. RNA was stored at -80°C.

RNA concentration was determined by diluting to 100-fold dilution in RNase/DNase-free water. The absorbance of diluted RNA was measured at 260 and 280 nm by spectrophotometer. An OD_{260} of 1.0 corresponds to a concentration of 40 μ g/ml single stranded RNA. Thus, the concentration of RNA was calculated by using the following equation.

$$\text{RNA (ug/ml)} = OD_{260} \times 40 \times \text{dilution factor}$$

The purification of RNA was measured from a ratio of OD_{260} / OD_{280} . The ratio of appropriately purified RNA was 1.8-2.0.

3.10 RT-PCR for mitochondrial gene expression in HeLa cells

3.10.1 cDNA synthesis

cDNA was synthesized by RNase-free DNase I reagent according to the manufacturer's instruction as follows: 1 ug of total RNA was incubated with 1u of RNase free DNase I in 1X DNase buffer at 37°C for 1 hour. Then, DNase I was inactivated by incubating with 2.5 mM EDTA at 65°C for 10 minutes. After that, 0.2 ug of random hexamer was added into DNase I-treated RNA. The mixture was incubated at 70°C for 5 minutes and chilled on ice. Then, 1X RT buffer, 1mM dNTP and 20 u of Ribonuclease inhibitor were added into the mixture and incubated at room temperature for 5 minutes. The final step of cDNA synthesis is the addition of 200 units of M-MuLV Reverse transcriptase into the mixture and incubated at 25°C for 10 minutes and 42°C for 1 hour, respectively. The reaction was stopped by heating at 70°C for 10 minutes. cDNA was stored at -80°C and used for PCR template.

3.10.2 PCR

Amplification of cDNA was carried out in sterilized 0.2 mL PCR tubes containing the mixture as follows: 1X PCR buffer, 1.5 mM $MgCl_2$, 200 uM dNTPs, 1 u Taq DNA polymerase, and 500 nM of each primer in 25 μ L reaction. The primer sequences and PCR product sizes(18) were shown in the Table 3.

3.10.2.1 PCR for Glyceraldehyde 3 phosphate dehydrogenase expression

PCR for glyceraldehyde 3 phosphate dehydrogenase was performed using the following condition: initial heat denaturation at 95°C for 5 minutes and 25 cycles of heat denaturation at 95°C for 30 seconds, primer annealing at 60°C for 30 seconds and DNA extension at 72°C for 30 seconds. Elongation step was extended at 72°C for 5 minutes.

3.10.2.2 PCR for ATP synthase expression

PCR for ATP synthase was performed using the following condition: initial heat denaturation at 95°C for 5 minutes and 25 cycles of heat denaturation at 95°C for 30 seconds, primer annealing at 60°C for 30 seconds and DNA extension at 72°C for 30 seconds. Elongation step was extended at 72°C for 5 minutes.

3.10.2.3 PCR for Cyt b expression

PCR for Cyt b was performed using the following condition: initial heat denaturation at 95°C for 5 minutes and 25 cycles of heat denaturation at 95°C for 30 seconds, primer annealing at 60°C for 30 seconds and DNA extension at 72°C for 30 seconds. Elongation step was extended at 72°C for 5 minutes.

3.10.2.4 PCR for CO1 expression

PCR for CO1 was performed using the following condition: initial heat denaturation at 95°C for 5 minutes and 25 cycles of heat denaturation at 95°C for 30 seconds, primer annealing at 60°C for 30 seconds and DNA extension at 72°C for 30 seconds. Elongation step was extended at 72°C for 5 minutes.

3.10.2.5 PCR for CO2 expression

PCR for CO2 was performed using the following condition: initial heat denaturation at 95°C for 5 minutes and 25 cycles of heat denaturation at 95°C for 30 seconds, primer annealing at 60°C for 30 seconds and DNA extension at 72°C for 30 seconds. Elongation step was extended at 72°C for 5 minutes.

3.10.2.6 PCR for ND3 expression

PCR for ND3 was performed using the following condition: initial heat denaturation at 95°C for 5 minutes and 25 cycles of heat denaturation at 95°C for 30 seconds, primer annealing at 60°C for 30 seconds and DNA extension at 72°C for 30 seconds. Elongation step was extended at 72°C for 5 minutes.

3.10.3 Agarose gel electrophoresis

Agarose gel electrophoresis was done to visualize the PCR products as follows: 1.5% agarose gel was prepared by mixing 0.6 grams of agarose powder with 40 mL of 1X TAE buffer. The agarose powder was melted in a microwave oven. Agarose was poured into a casting tray containing a sample comb and allowed to set at room temperature for 30 minutes. The gel was inserted horizontally into the electrophoresis chamber. Samples containing 5 µL of DNA mixed with loading buffer were pipetted into the wells, the lid and power lines were placed on the apparatus and a current was applied. The gel was run in 1X TAE buffer at 100 volt for 40 minutes. After the agarose gel electrophoresis was done, the gel was stained in ethidium bromide and the gel images were captured by Gel Document. The band density was measured by the Quantity One program for calculated the concentration and area by compared with the reference band (DNA ladder).

Table 3 Primer sequences and PCR product sizes

Gene	Primer	PCR product
GAPDH-Forward	CCATGGCACCGTCAAGGCTGA	151 bp
GAPDH-Reverse	CTCCATGGTGGTGAAGACGC	
CO1- Forward	TACGTTGTAGCCCACTTCCACT	189 bp
CO1- Reverse	GGATAGGCCGAGAAAGTGTGT	
CO2- Forward	GTAGTACTCCCGATTGAAGCCC	214 bp
CO2- Reverse	ATTCTAGGACGATGGGCATGAA	
ATP synthase- Forward	CCATCAGCCTACTCATTCAACC	184 bp
ATP synthase- Reverse	GCGACAGCGATTTCTAGGATAG	
ND3- Forward	CCACAACCTCAACGGCTACATAG	245 bp
ND3- Reverse	CACTCATAGGCCAGACTTAGGG	
Cyt b- Forward	TATTCGCCTACACAATTCTCCG	209 bp
Cyt b- Reverse	GCTTACTGGTTGTCCTCCGATT	

ศูนย์วิทยทรัพยากร
จุฬาลงกรณ์มหาวิทยาลัย

CHAPTER IV

RESULTS AND DISCUSSION

4.1 Characterization of Gold Nanoparticles

The citrate-stabilized gold nanoparticles are characterized by UV-Vis spectrophotometer and Transmission Electron Microscopy (TEM). The result of absorption spectrum of gold nanoparticles is shown in Figure 11. The plasmon wavelength (λ_{\max}) indicates the size of gold nanoparticles and plasmon width ($\Delta\lambda$) indicates the size distribution of gold nanoparticles that are their unique properties. In this present study, the λ_{\max} and $\Delta\lambda$ of gold nanoparticles are approximately at 520 nm and 95 nm, respectively. These values relate to the color of colloidal gold nanoparticles which observed by naked eyes.

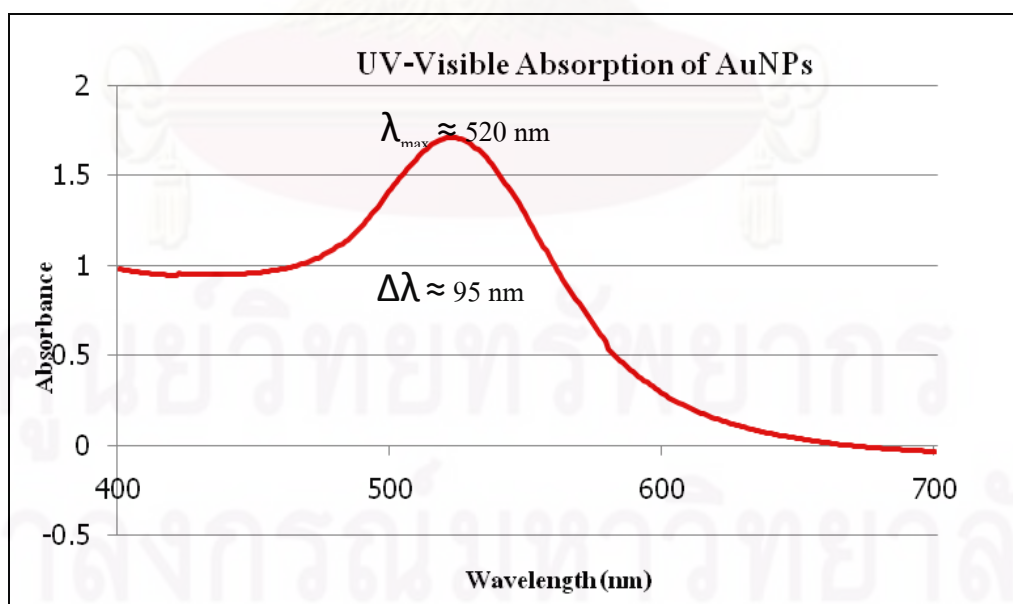


Figure 11 The characterization of gold nanoparticles using spectrophotometer. The absorption spectrum of gold nanoparticles have $\lambda_{\max} \approx 520 \text{ nm}$ and $\Delta\lambda \approx 95 \text{ nm}$.

These values of citrate-stabilized gold nanoparticles are similar with other different synthetic methods, reviewed by Daniel(25). The red shift in λ_{\max} is associated with an increase in the mean size of the gold nanoparticles or modification in the surrounding media. Moreover, any change in $\Delta\lambda$ indicates an aggregation of gold nanoparticles or modification in the surrounding media.

Further characterization of gold nanoparticles, a Transmission Electron Microscope (TEM) was used for determining the size and size distribution of citrate-stabilized gold nanoparticles. The size and size distribution of citrate-stabilized gold nanoparticles are shown in Figure 12. TEM images show that the diameter of spherical gold nanoparticles range from 10 to 15 nm with monodisperse size distribution.

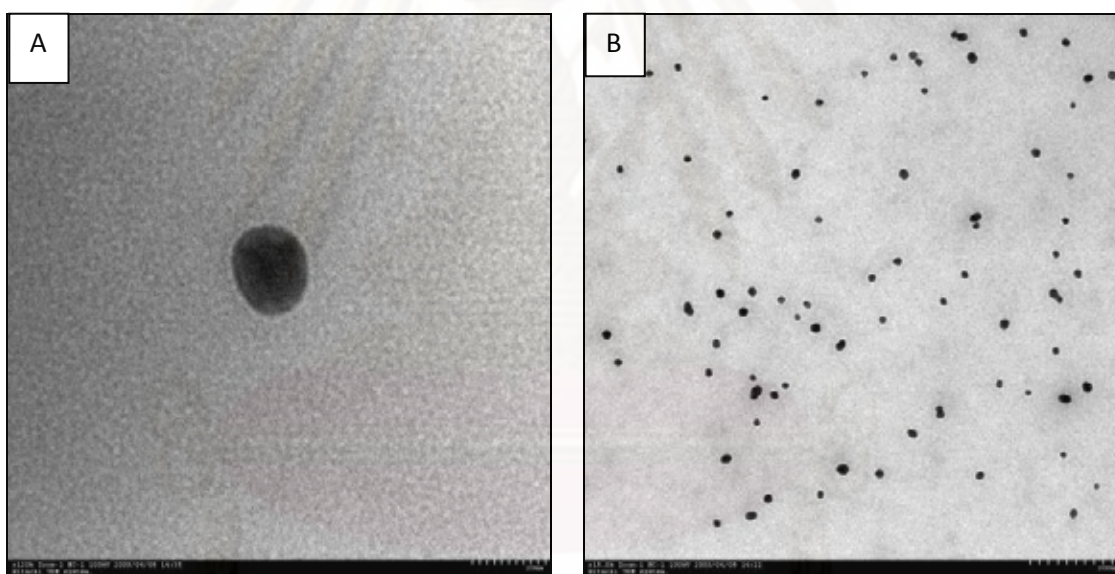


Figure 12 The characterization of gold nanoparticles using TEM. Fig 13A shows a spherical gold nanoparticles which have an average size at 10-15 nm. Fig 13B shows the monodisperse size distribution of gold nanoparticles.

The size and shape of synthesized gold nanoparticles are similar to the citrate reduction of HAuCl_4 in water, which was introduced by Turkevitch(26). This method leads to 10-20 nm spherical gold nanoparticles with monodisperse size distribution.

4.2 Effects of gold nanoparticles on cell morphology

The cell morphology of HeLa cells in the presence of gold nanoparticles was investigated using Light Microscope (LM). After incubation of gold nanoparticles with various concentrations of citrate-stabilized gold nanoparticles, cell morphology of HeLa cells was observed and photographs were taken. Cell morphology of HeLa cells in gold nanoparticles treated groups was compared with negative and positive control groups, as shown in figure 13 and 14. In negative control groups, HeLa cells were cultured in the media for 1, 2 and 3 days, whereas positive control groups, HeLa cells were incubated with DMSO.



In the negative control, cells were able to continuously grow until the third day with increasing cell proliferation. The HeLa cells morphology is well spread and attach on the plate, as shown in figure 13.

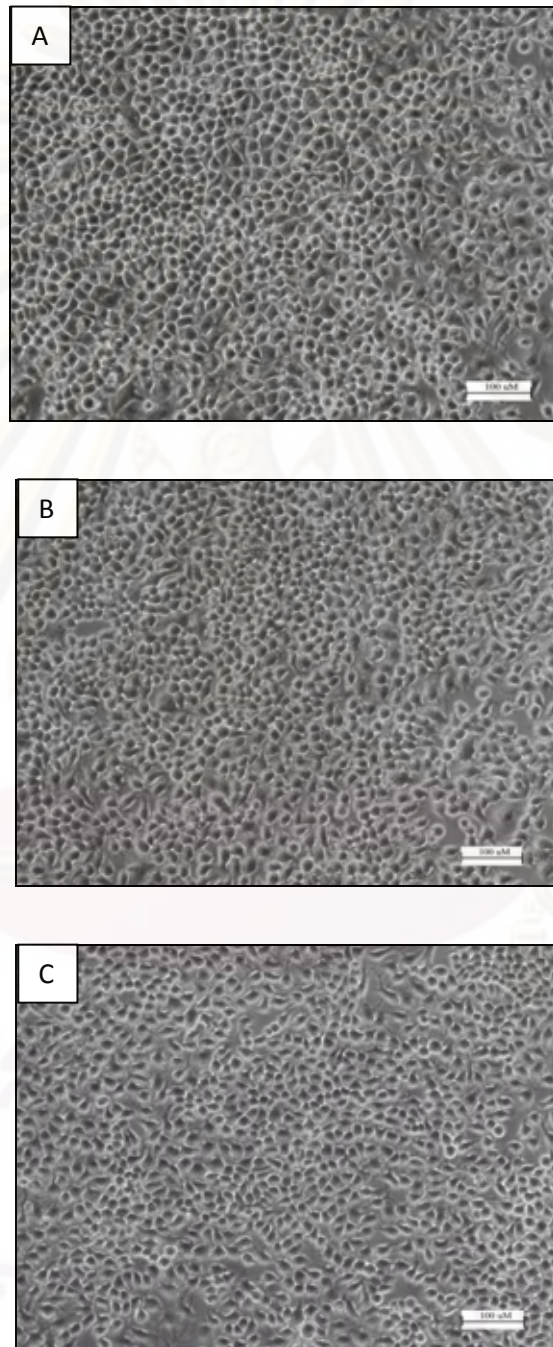


Figure 13 General cell morphology in negative control. The cultivation of HeLa cells alone for 1, 2 and 3 days (A-C).

HeLa cells morphology in positive groups is shown in figure 14. The decreasing cell proliferation and cell adhesion were obviously observed. These results indicated the characteristic of cell death.

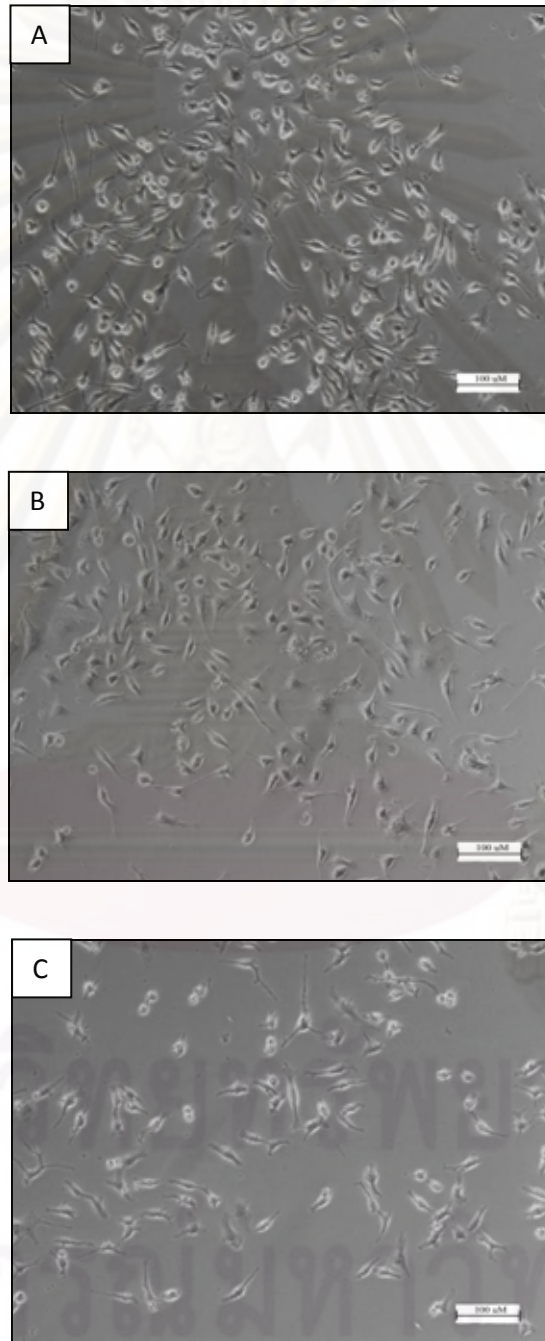


Figure 14 HeLa cells morphology in positive control. The incubation of HeLa cells with DMSO for 1, 2 and 3 days (A-C).

HeLa cells morphology in the presence of citrate is shown in figure 15, there was no distinct change in morphology could be observed.

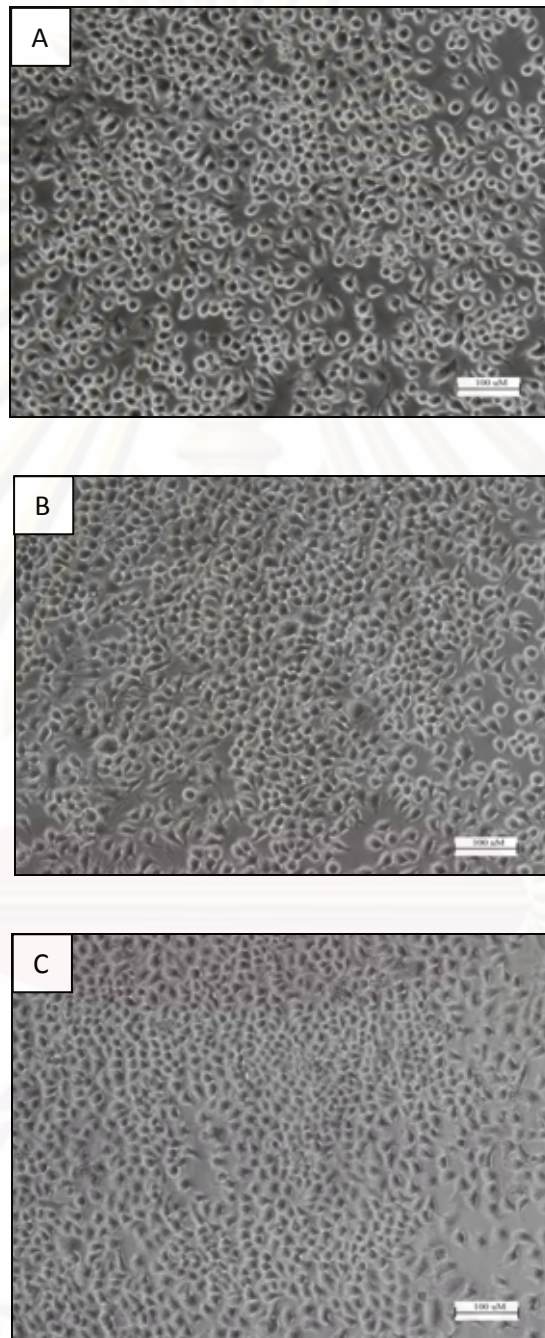


Figure 15 HeLa cells morphology in the presence of citrate. The incubation of HeLa cells with citrate for 1, 2 and 3 days (A-C).

HeLa cells morphology in the presence of 10 ug/mL gold nanoparticles is shown in figure 16, morphological changes were not observed after incubation for 1, 2 and 3 days.

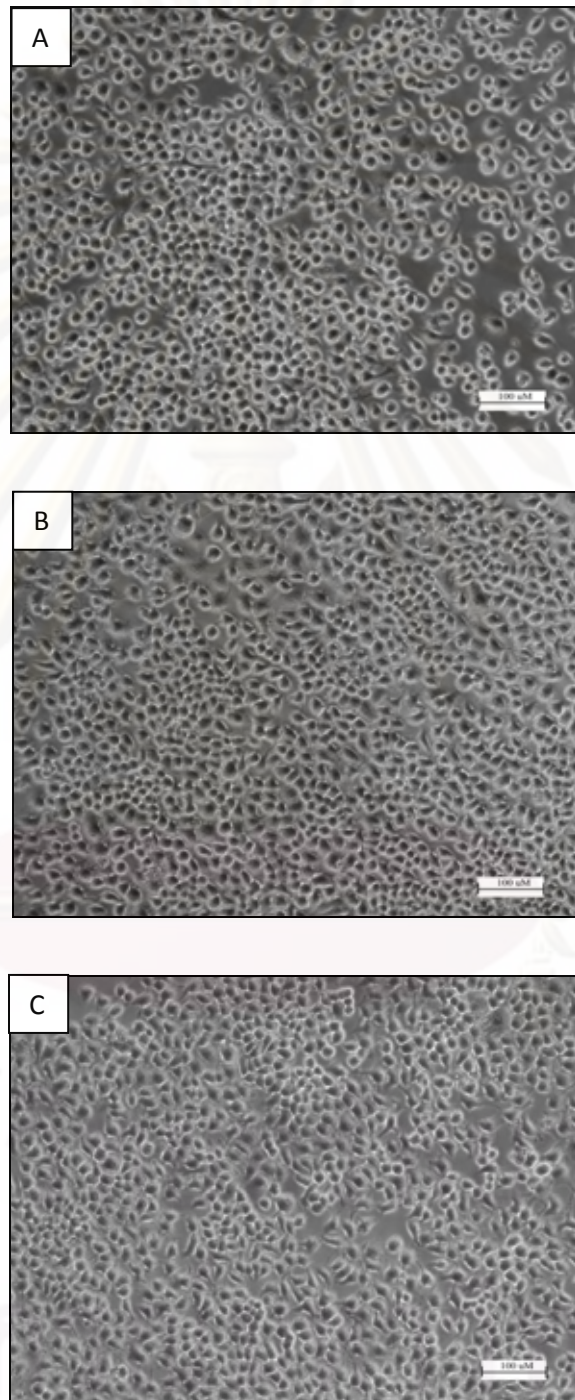


Figure 16 HeLa cells morphology in the presence of 10 ug/mL gold nanoparticles. The incubation of HeLa cells with 10 ug/mL gold nanoparticles for 1, 2 and 3 days (A-C).

HeLa cells morphology in the presence of 50 ug/mL gold nanoparticles is shown in figure 17, morphological changes were not found.

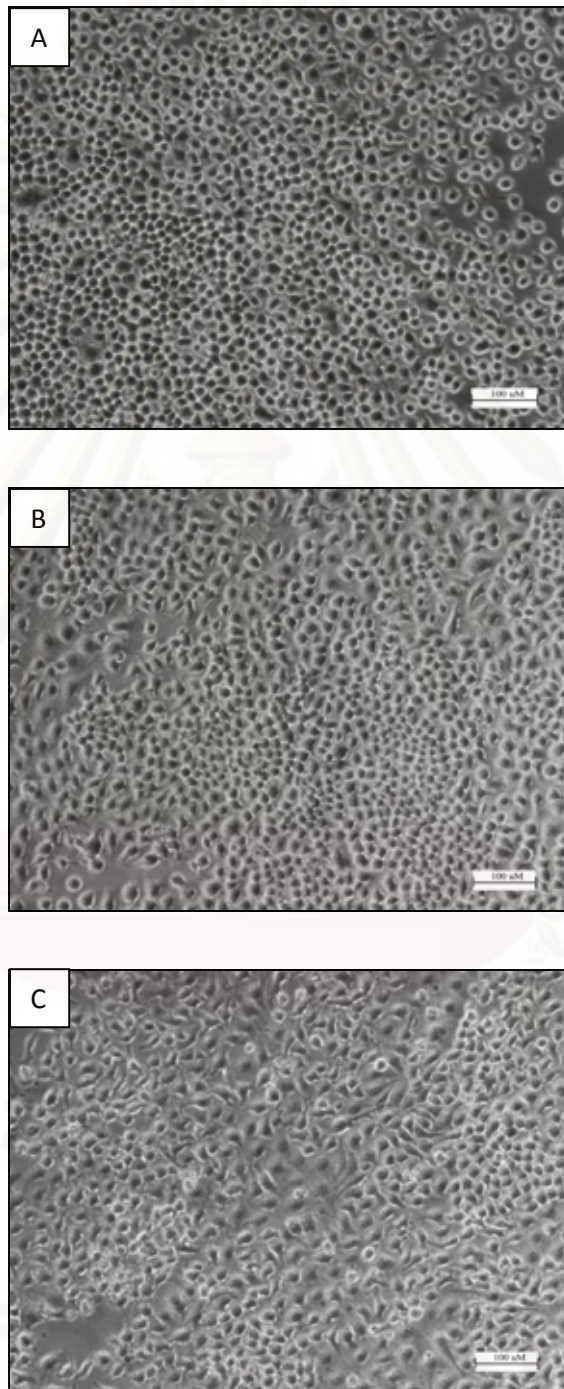


Figure 17 HeLa cells morphology in the presence of 50 ug/mL gold nanoparticles. The incubation of HeLa cells with 50 ug/mL gold nanoparticles for 1, 2 and 3 days (A-C).

HeLa cells morphology in the presence of 100 ug/mL gold nanoparticles is shown in figure 18, morphological changes were observed. The cells become shrink and irregular after third day incubation with gold nanoparticles.

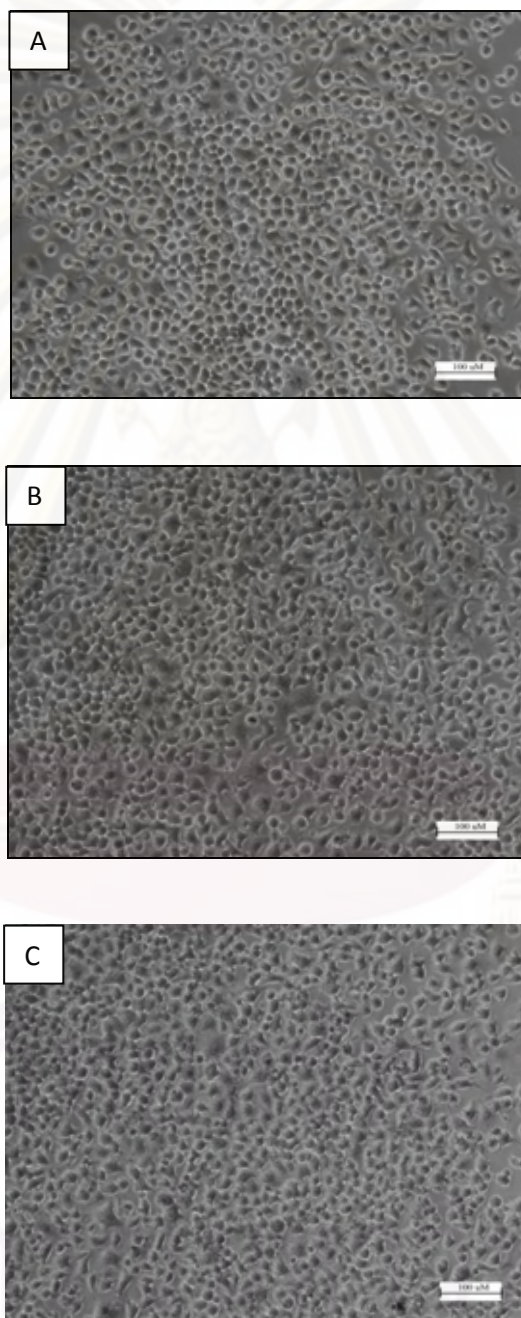


Figure 18 HeLa cells morphology in the exposure to 100 ug/mL gold nanoparticles. The incubation of HeLa cells with 100 ug/mL gold nanoparticles for 1, 2 and 3 days (A-C).

These experiments show that the cells were well spread and there was no distinct change in morphology after the incubation with 10 and 50 ug/mL of gold nanoparticles relative to untreated cells. However, dramatic changes occurred with 100 ug/mL gold nanoparticles treated group in the third day. The cells become irregular, contract and detach. Thus, 100 ug/mL gold nanoparticles is considered as the toxic concentration for cells. It could be concluded that the dramatic changes induced by an increasing gold nanoparticles concentration and incubation time. This information should be considered for further in vivo application of gold nanoparticles.

These findings are in agreement with Pernodet(35) who reported the dose-dependent cytotoxicity. The contracted fibroblast cells and decreasing cell proliferation were observed. They suggested that cytoskeleton is affected in the presence of citrate-stabilized gold nanoparticles.

4.3 *In Vitro* Cytotoxicity

The effect of various concentrations of citrate-stabilized gold nanoparticles on HeLa cell viability was examined using MTT assay. After 1, 2 and 3 days incubation, no effect on 10 and 50 ug/mL gold nanoparticles treated groups could be observed. In contrast, the 100 ug/mL gold nanoparticles treated groups in the third day exhibited significantly toxicity. These results were compared to the control groups, as shown in figure 19. Moreover, the survival of the HeLa cells also decreased in the presence of citrate. The results show that 10 and 50 ug/mL concentration of gold nanoparticles exhibit non-toxic, except the concentrations of 100 ug/mL. It was observed that cell viability following exposure to gold nanoparticles was dependent on concentration and time incubation.

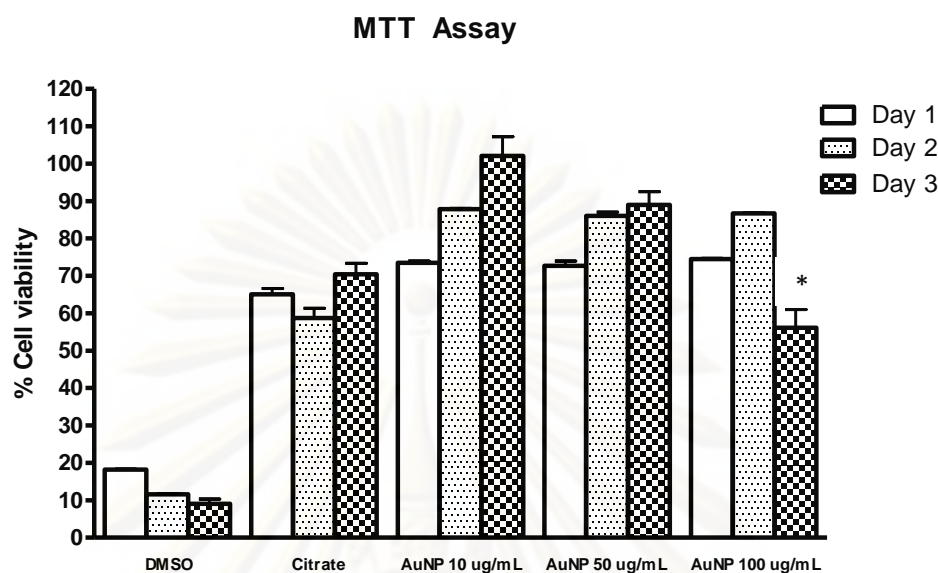


Figure 19 The influence of gold nanoparticles on cell viability. HeLa cells were exposed to DMSO, citrate and 10, 50, 100 ug/mL gold nanoparticles for 1, 2 and 3 days. The values reported in this graphs are the average of triplicate samples. Vertical lines denote \pm 1SD (n=3). Significant of differences between dose and time: *, p-value<0.05).

Gold nanoparticles at the concentration of 10 and 50 ug/mL do not affect on HeLa cells, whereas 100 ug/mL gold nanoparticles exhibit cytotoxicity. These findings are in agreement with many recent previous results which reported that increasing concentration lead to increase in cytotoxicity. Our results implied that longer than 3 days incubation with 100 ug/mL gold nanoparticles can further decrease cell viability. Interestingly the HeLa cell showed greater sensitivity to 9.7 mM trisodium citrate than gold nanoparticles, which suggests that surface modification can generate cytotoxicity on HeLa cells. However, in the case of Connor(15) and Khan(16) and Tkachenko(32), they found that there are no significant differences in viability levels for gold nanoparticles at various concentrations, times and cell lines.

4.3 Localization of gold nanoparticles

The fate and localization of gold nanoparticles were investigated using TEM. Moreover, the influence of gold nanoparticles on morphological intracellular organelles was also examined. It was found that gold nanoparticles were readily taken up by the HeLa cells and ended up in the endosome, as shown in Figure 20.

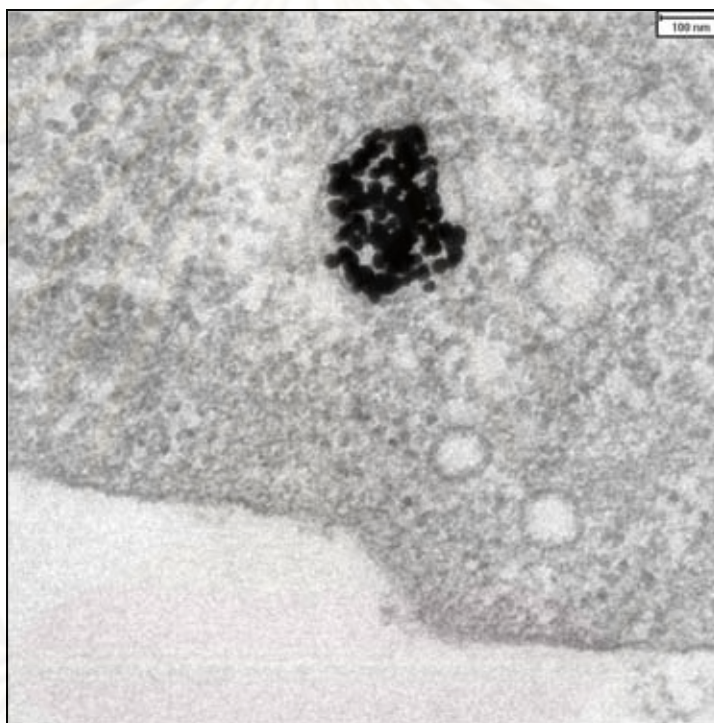


Figure 20 Cellular uptake of 10-15 nm gold nanoparticles via the endocytosis.

Inside the cell, most of gold nanoparticles are found in the endosomes, but gold nanoparticles are also observed freely dispersed in the cytosol. In addition, gold nanoparticles were aggregated close to but not in the mitochondria or nucleus, as illustrated in Figure 21. The results demonstrate that gold nanoparticles are indeed in the cytosol.

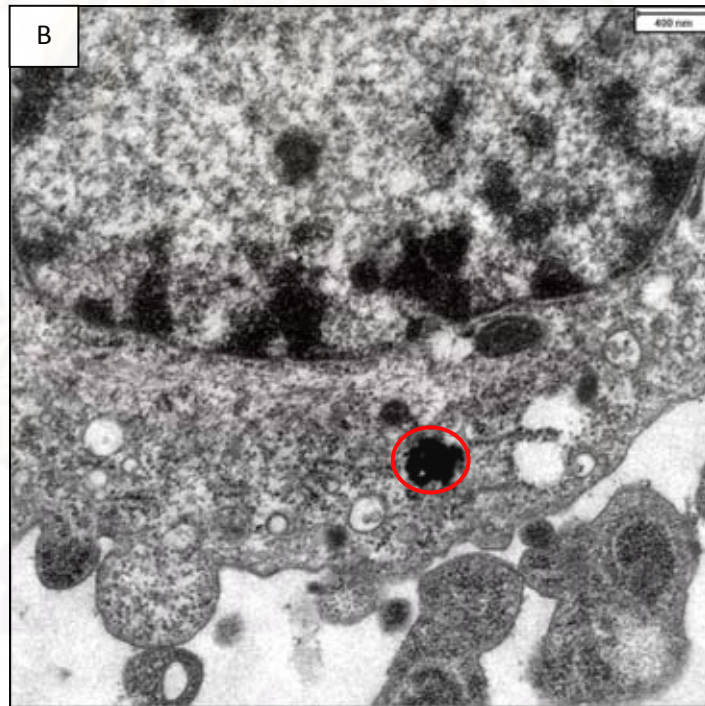
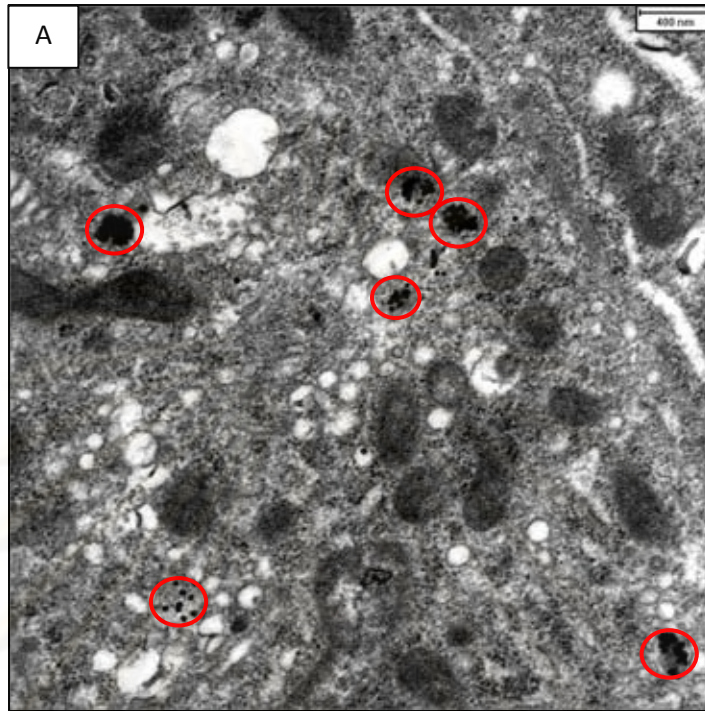


Figure 21 Internalization of gold nanoparticles. Fig 21A demonstrates that gold nanoparticles were freely dispersed in the cytosol. Fig 21B shows gold nanoparticles were aggregated close to but not in the mitochondria or nucleus.

The results of cells exposed to gold nanoparticles showed that nucleus, mitochondria and ER were not affected morphologically (figure 22).

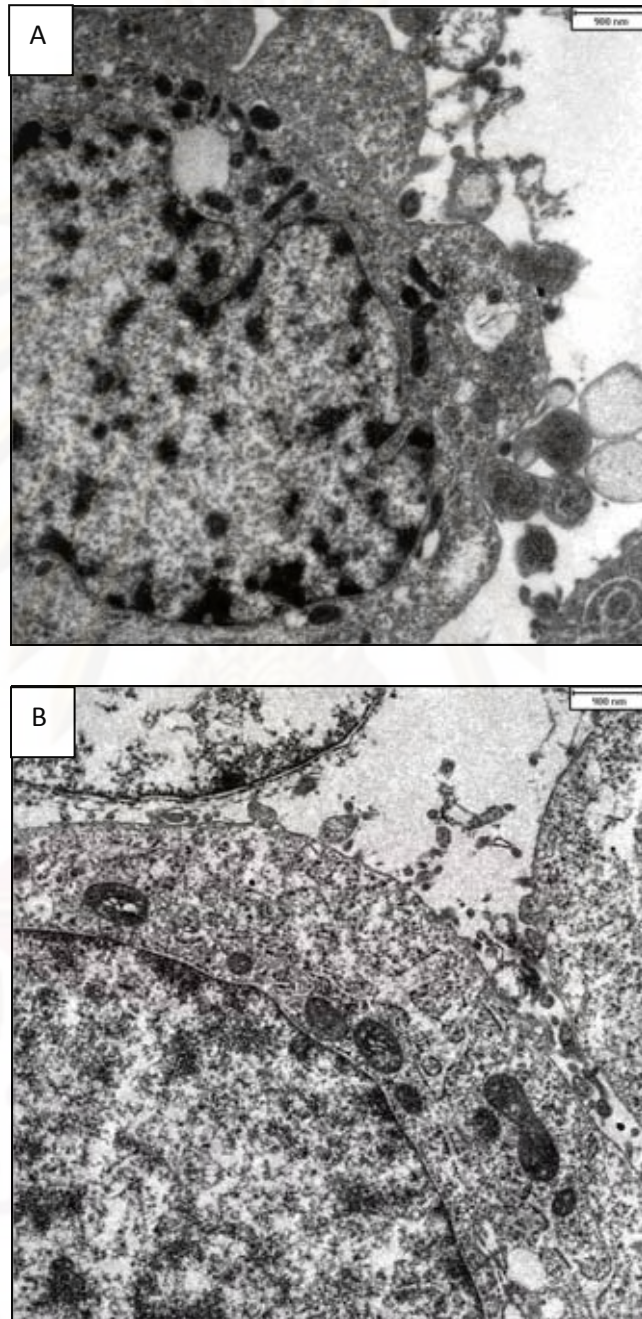
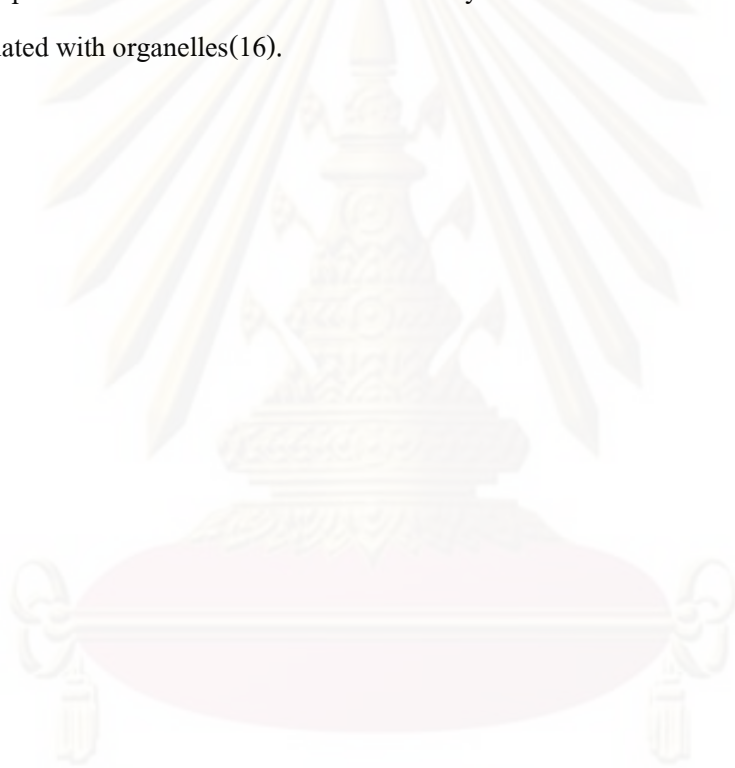


Figure 22 Intracellular organelles morphology. Fig 22A shows the nuclei, mitochondria and ER were not altered in the exposure to gold nanoparticles. Fig 22B indicates the general morphology of intracellular organelles.

Finally, gold nanoparticles can not penetrate nuclear membranes and attach to DNA consequently; gold nanoparticles can not cause toxicity. These findings confirm the nontoxic nature of gold nanoparticles, which enter the cells but do not affect nucleus, mitochondria and ER. Cellular uptake of gold nanoparticles is similar to previous studies. Connor *et al.* report 18 nm citrate-stabilized gold nanoparticles are taken up by K562 cells but do not cause cytotoxicity after 24 hours incubation(15). Moreover, Khan *et al.* reported 18 nm gold nanoparticles (2 nM) were trapped in vesicles and internalized inside HeLa cells after 6 hours incubation. Even after a longer incubation time, the nanoparticles did not enter the nucleus. They localized within the cytoplasm, but were not closely associated with organelles(16).



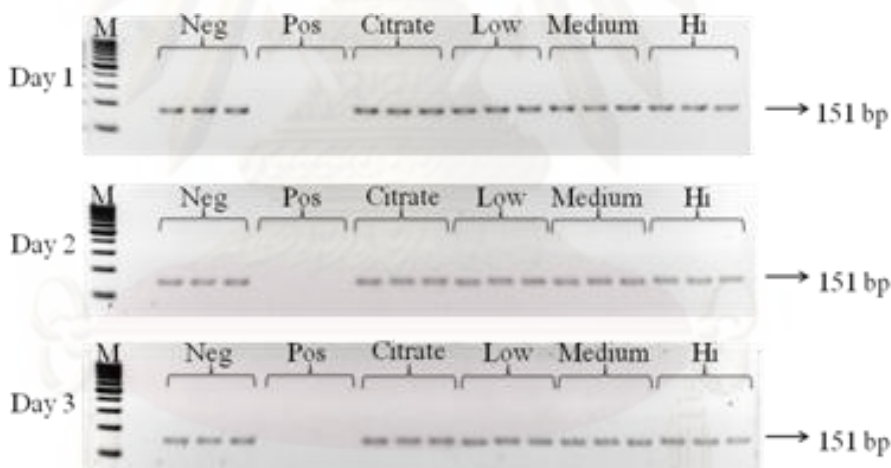
ศูนย์วิทยทรัพยากร
จุฬาลงกรณ์มหาวิทยาลัย

4.4 Mitochondrial gene expression

4.4.1 Glyceraldehyde-3-phosphate dehydrogenated (GAPDH) expression

GAPDH is an enzyme in cellular glycolytic pathway that is the most widely used as housekeeping gene in RT-PCR experiment. Because of its consistency of expression, housekeeping gene was used to normalize the targeted gene (ATP synthase, cytochrome b, cytochrome c oxidase 1, cytochrome c oxidase 2 and NADH dehydrogenase 3) expression.

RT-PCR for GAPDH expression was done to demonstrate successful RNA extraction. The 151-bp PCR product indicates GAPDH gene expression was detected in all samples. However, the positive groups (DMSO-treated HeLa cells) were not detected (Figures 23). The demonstrated data were derived from 3 replicated samples.



Neg=No AuNP, Pos=DMSO 100 uL, Citrate=trisodium citrate solution 100 uL, Low=AuNP 10 ug/mL, Medium=50 ug/mL, Hi=100 ug/mL

Figure 23 GAPDH mRNA expression in all samples. cDNA was transcribed from RNA extracted from HeLa cells and PCR using GAPDH primers was performed as described in Materials and Methods. Lane M : 100-bp marker; Lane 1 : negative control; Lane 2, 3, 4 : RNA extracted from the cultivation of HeLa cells alone; Lane 5, 6, 7 : RNA extracted from DMSO-treated HeLa cells; Lane 8, 9, 10 : RNA extracted from citrate-treated HeLa cells; Lane 11, 12, 13 : RNA extracted from 10 ug/mL AuNPs-treated HeLa cells; Lane 14, 15, 16 : RNA extracted from 50 ug/mL AuNPs-treated HeLa cells; Lane 17, 18, 19 : RNA extracted from 100 ug/mL AuNPs-treated HeLa cells.

4.4.2 ATP synthase expression

The 184-bp PCR product indicated the presence of ATP synthase mRNA gene expression. ATP synthase mRNA expression was detected in all samples, whereas the positive groups (DMSO-treated HeLa cells) were not detected (Figures 24).

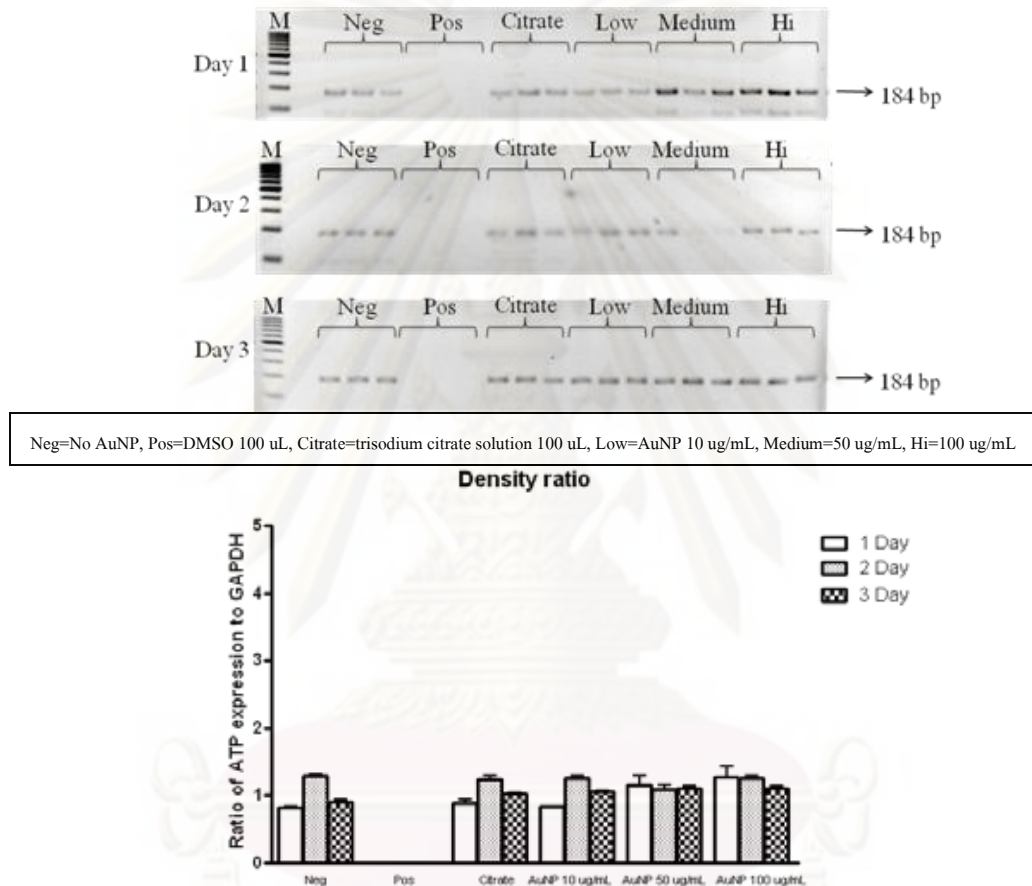


Figure 24 ATP synthase mRNA expression in all samples. cDNA was transcribed from RNA extracted from HeLa cells and PCR using ATP synthase primers was performed as described in Materials and Methods. Lane M : 100-bp marker; Lane 1 : negative control; Lane 2, 3, 4 : RNA extracted from the cultivation of HeLa cells alone; Lane 5, 6, 7 : RNA extracted from DMSO-treated HeLa cells; Lane 8, 9, 10 : RNA extracted from citrate-treated HeLa cells; Lane 11, 12, 13 : RNA extracted from 10 ug/mL AuNPs-treated HeLa cells; Lane 14, 15, 16 : RNA extracted from 50 ug/mL AuNPs-treated HeLa cells; Lane 17, 18, 19 : RNA extracted from 100 ug/mL AuNPs-treated HeLa cells. The graph underneath figure demonstrates density ratio between bands from ATPase and GAPDH PCR products.

4.4.3 Cytochrome B (Cyt B) expression

The 209-bp PCR product indicated the presence of Cytochrome B mRNA gene expression. Cytochrome B mRNA expression was detected in all samples, whereas the positive groups (DMSO-treated HeLa cells) were not detected (Figures 25).

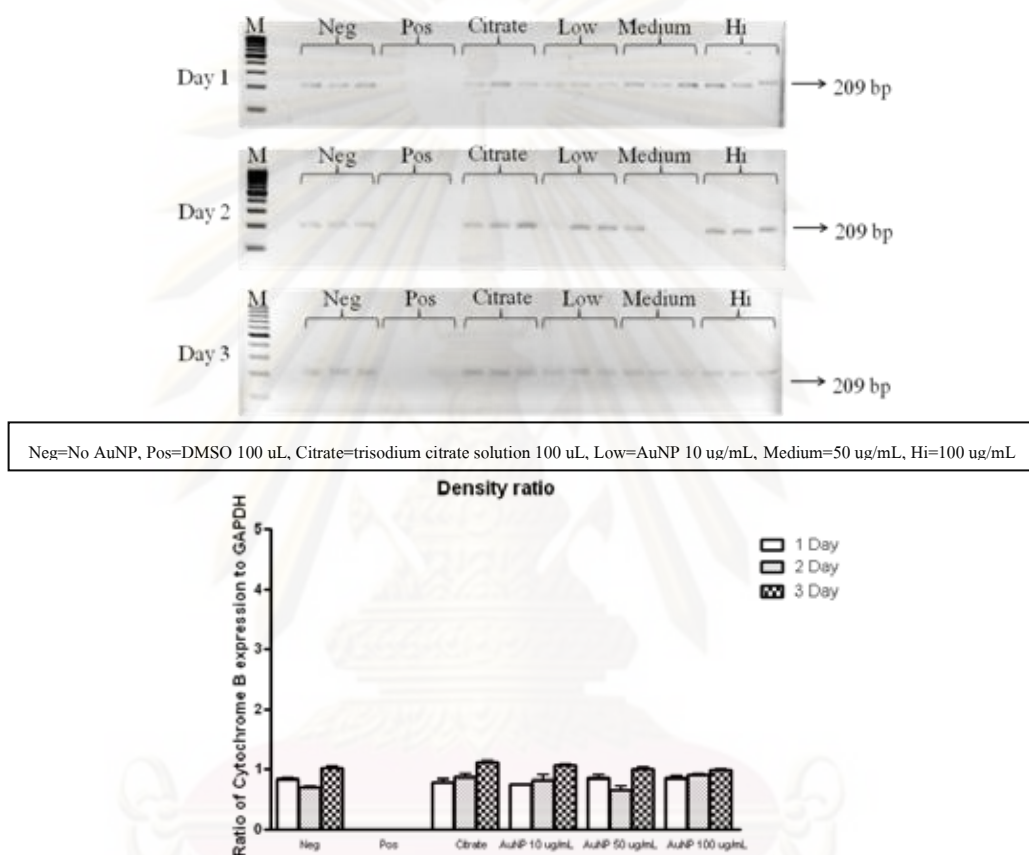


Figure 25 Cytochrome B mRNA expression in all samples. cDNA was transcribed from RNA extracted from HeLa cells and PCR using Cytochrome B primers was performed as described in Materials and Methods. Lane M : 100-bp marker; Lane 1 : negative control; Lane 2, 3, 4 : RNA extracted from the cultivation of HeLa cells alone; Lane 5, 6, 7 : RNA extracted from DMSO-treated HeLa cells; Lane 8, 9, 10 : RNA extracted from citrate-treated HeLa cells; Lane 11, 12, 13 : RNA extracted from 10 ug/mL AuNPs-treated HeLa cells; Lane 14, 15, 16 : RNA extracted from 50 ug/mL AuNPs-treated HeLa cells; Lane 17, 18, 19 : RNA extracted from 100 ug/mL AuNPs-treated HeLa cells. The graph underneath figure demonstrates density ratio between bands from Cytochrome B and GAPDH PCR products.

4.4.4 Cytochrome C Oxidase 1 (CO1) expression

The 189-bp PCR product indicated the presence of Cytochrome C Oxidase 1 mRNA gene expression. Cytochrome C Oxidase 1 mRNA expression was detected in all samples, whereas the positive groups (DMSO-treated HeLa cells) were not detected (Figures 26).

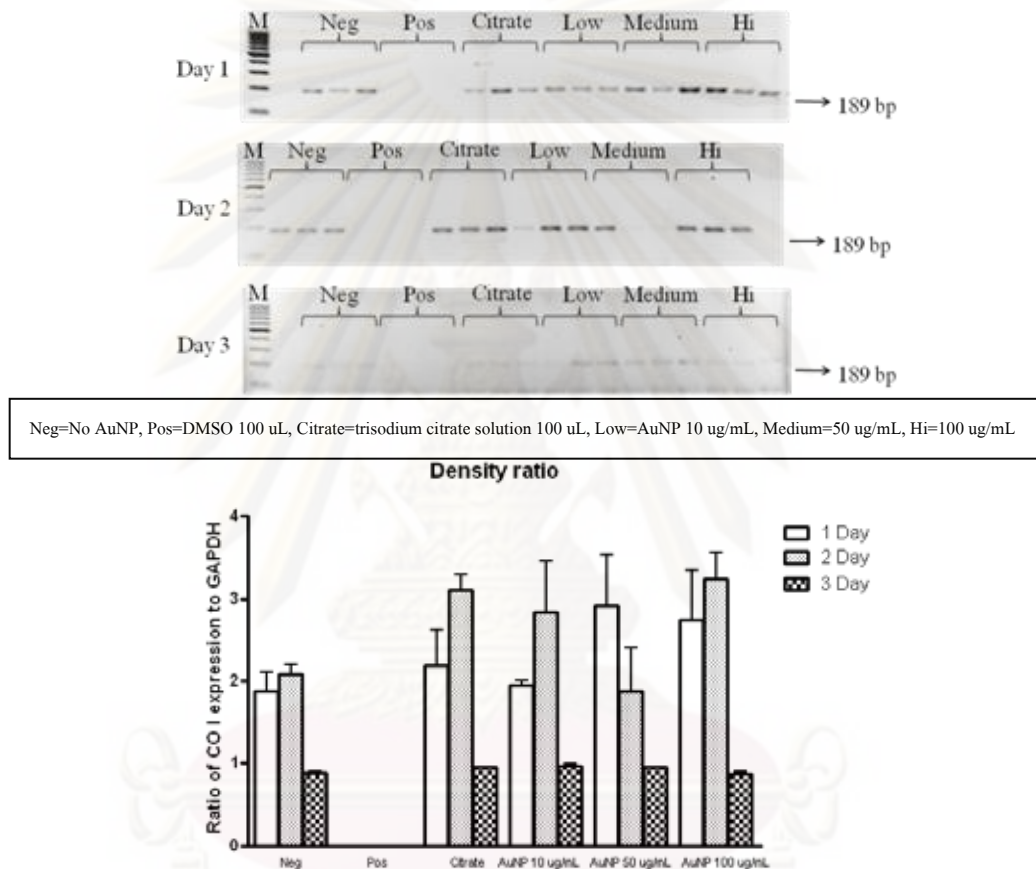


Figure 26 Cytochrome C Oxidase 1 mRNA expression in all samples. cDNA was transcribed from RNA extracted from HeLa cells and PCR using Cytochrome C Oxidase 1 primers was performed as described in Materials and Methods. Lane M : 100-bp marker; Lane 1 : negative control; Lane 2, 3, 4 : RNA extracted from the cultivation of HeLa cells alone; Lane 5, 6, 7 : RNA extracted from DMSO-treated HeLa cells; Lane 8, 9, 10 : RNA extracted from citrate-treated HeLa cells; Lane 11, 12, 13 : RNA extracted from 10 ug/mL AuNPs-treated HeLa cells; Lane 14, 15, 16 : RNA extracted from 50 ug/mL AuNPs-treated HeLa cells; Lane 17, 18, 19 : RNA extracted from 100 ug/mL AuNPs-treated HeLa cells. The graph underneath figure demonstrates density ratio between bands from Cytochrome C Oxidase I and GAPDH PCR products.

4.4.5 Cytochrome C Oxidase 2 (CO2) expression

The 214-bp PCR product indicated the presence of Cytochrome C Oxidase 2 mRNA gene expression. Cytochrome C Oxidase 2 mRNA expression was detected in all samples, whereas the positive groups (DMSO-treated HeLa cells) were not detected (Figures 27).

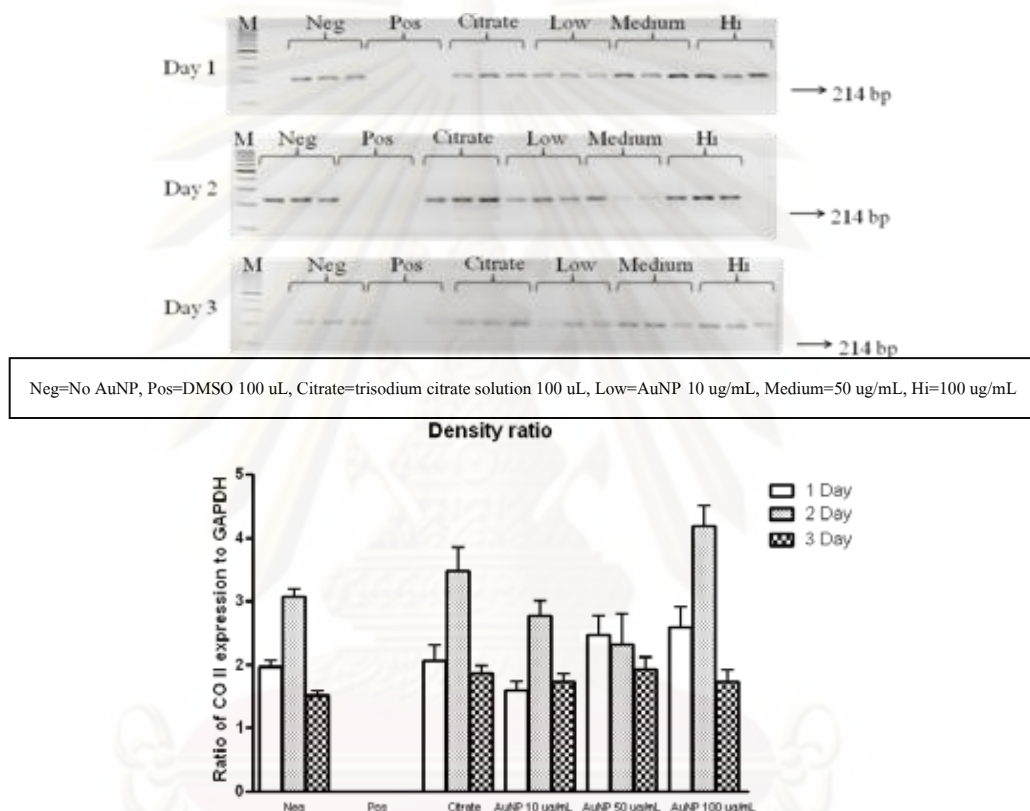


Figure 27 Cytochrome C Oxidase 2 mRNA expression in all samples. cDNA was transcribed from RNA extracted from HeLa cells and PCR using Cytochrome C Oxidase 2 primers was performed as described in Materials and Methods. Lane M : 100-bp marker; Lane 1 : negative control; Lane 2, 3, 4 : RNA extracted from the cultivation of HeLa cells alone; Lane 5, 6, 7 : RNA extracted from DMSO-treated HeLa cells; Lane 8, 9, 10 : RNA extracted from citrate-treated HeLa cells; Lane 11, 12, 13 : RNA extracted from 10 ug/mL AuNPs-treated HeLa cells; Lane 14, 15, 16 : RNA extracted from 50 ug/mL AuNPs-treated HeLa cells; Lane 17, 18, 19 : RNA extracted from 100 ug/mL AuNPs-treated HeLa cells. The graph underneath figure demonstrates density ratio between bands from Cytochrome C Oxidase II and GAPDH PCR products.

4.4.6 NADH Dehydrogenase 3 (ND3) expression

The 245-bp PCR product indicated the presence of NADH Dehydrogenase 3 mRNA gene expression. NADH Dehydrogenase 3 mRNA expression was detected in all samples, whereas the positive groups (DMSO-treated HeLa cells) were not detected (Figures 28).

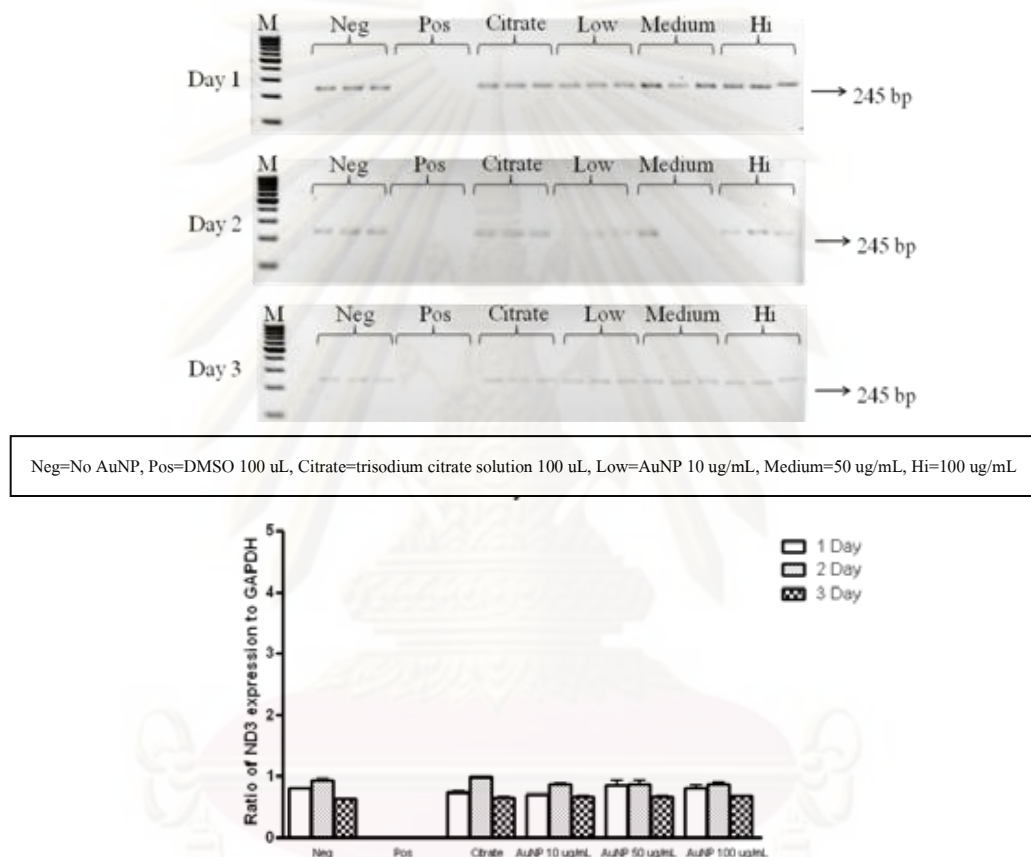
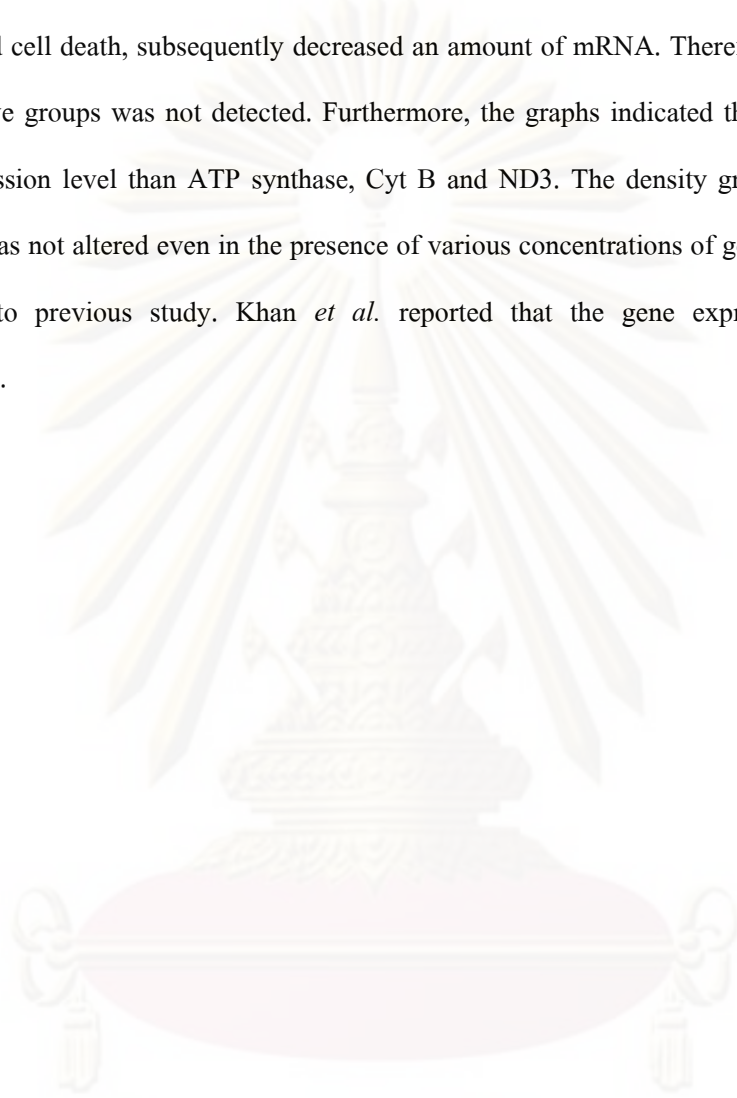


Figure 28 NADH Dehydrogenase 3 mRNA expression in all samples. cDNA was transcribed from RNA extracted from HeLa cells and PCR using NADH Dehydrogenase 3 primers was performed as described in Materials and Methods. Lane M : 100-bp marker; Lane 1 : negative control; Lane 2, 3, 4 : RNA extracted from the cultivation of HeLa cells alone; Lane 5, 6, 7 : RNA extracted from DMSO-treated HeLa cells; Lane 8, 9, 10 : RNA extracted from citrate-treated HeLa cells; Lane 11, 12, 13 : RNA extracted from 10 ug/mL AuNPs-treated HeLa cells; Lane 14, 15, 16 : RNA extracted from 50 ug/mL AuNPs-treated HeLa cells; Lane 17, 18, 19 : RNA extracted from 100 ug/mL AuNPs-treated HeLa cells. The graph underneath figure demonstrates density ratio between bands from NADH Dehydrogenase 3 and GAPDH PCR products.

The results show that gene expression could be detected in all samples except the positive groups. In the positive groups, HeLa cells were incubated with DMSO, a well known toxic agent, which caused cell death, subsequently decreased an amount of mRNA. Therefore, mRNA expression in the positive groups was not detected. Furthermore, the graphs indicated that CO1 and CO2 have higher expression level than ATP synthase, Cyt B and ND3. The density graphs showed that gene expression was not altered even in the presence of various concentrations of gold nanoparticles which are similar to previous study. Khan *et al.* reported that the gene expression level remained unaltered(16).



ศูนย์วิทยทรัพยากร
จุฬาลงกรณ์มหาวิทยาลัย

CHAPTER V

CONCLUSION

In brief, this study reports that low to moderate concentrations (10 and 50 $\mu\text{g/mL}$, respectively) of gold nanoparticles were not affected cell viability and cell proliferation, whereas high gold nanoparticles concentration (100 $\mu\text{g/mL}$) reduced cell viability. In addition, increase incubation time together with high concentration of AuNP caused a drastic decrease in cell viability.

Cell morphology was altered after 3 day incubation with 100 $\mu\text{g/mL}$ gold nanoparticles. High concentration of gold nanoparticles induced irregular cell morphology and cell shrinkage, while 10, 50 $\mu\text{g/mL}$ gold nanoparticles are non-toxic to adherent epithelial cells.

By using transmission electron microscope, the examination of intracellular localization revealed that 10-15 nm gold nanoparticles infiltrated cell membrane and localized into cytoplasm, with no evidence of intranuclear penetration. Gold nanoparticles appear to be internalized within the endosome.

The mitochondrial gene expression level was not significantly altered in the presence of 10-15 nm-sized gold nanoparticles at the various concentrations in HeLa cells.

ศูนย์วิจัยทรัพยากร
จุฬาลงกรณ์มหาวิทยาลัย

CHAPTER VI

FUTURE PERSPECTIVE

Nanomedicine is promised to play a role in the development of diagnostic and therapeutic methods. In the near future, biomedical devices based on gold nanoparticles, which is the rapid, easy and inexpensive devices, will become available. Nevertheless, the environmental impact and health safety of gold nanoparticles should be concerned.

Nowadays, fundamental nanotoxicity/safety information has been evaluated using *in vitro* cytotoxicity assays, microscopes and gene expression profiles which have been used in many studies. These studies suggested that the appropriate incubation time and concentration of gold nanoparticles can be applied for *in vivo* biomedicine devices.

Gold nanoparticles seem to be an appropriate candidate since in many studies on different cells lines they are referred to be only slightly toxic. Despite, gold nanoparticles did not exhibit cytotoxicity but they could affect other organelle function and mechanism. Thus, the additional work could be done to more precisely determine the mechanism of cell destruction and the possible interactions and uptake/excretory mechanisms of these gold nanoparticles. These mechanisms could provide interesting information of gold nanoparticles toxicity.

Furthermore, the toxicity of surface functionalized gold nanoparticles has not been investigated. It would be interesting to determine if surface functionality has an affect on cell viability, cell morphology and mitochondrial genes expression.

REFERENCES

- [1] Roco MC. Nanotechnology: convergence with modern biology and medicine. Current Opinion in Biotechnology 14(2003): 337-346.
- [2] Oberdörster G, Maynard A, Donaldson K, Castranova V, Fitzpatrick J, Ausman K, et al. Principles for characterizing the potential human health effects from exposure to nanomaterials: elements of a screening strategy. Particle and Fibre Toxicology 2, 8 (2005).
- [3] Thomas K, Sayre P. Research Strategies for Safety Evaluation of Nanomaterials, Part I: Evaluating the Human Health Implications of Exposure to Nanoscale Materials. Toxicological Sciences 87, 2 (2005): 316-321.
- [4] Kell AJ, Donkers RL, Workentin MS. Core Size Effects on the Reactivity of Organic Substrates as Monolayers on Gold Nanoparticles. Langmuir 21 (2005): 735-742.
- [5] Xue C, Arumugam G, Palaniappan K, Hackney SA, Liu H, Liu J. Construction of conjugated molecular structures on gold nanoparticles via the Sonogashira coupling reactions. Chem Commun (2005): 1055-1057.
- [6] Ackerson CJ, Sykes MT, Kornberg RD. Defined DNA/nanoparticle conjugates. PNAS 102, 38 (2005): 13383-13385.
- [7] Storhoff JJ, Elghanian R, Mucic RC, Mirkin CA, Letsinger RL. One-Pot Colorimetric Differentiation of Polynucleotides with Single Base Imperfections Using Gold Nanoparticle Probes. J Am Chem Soc 120 (1998): 1959-1964.
- [8] Letsinger RL, Mirkin CA, Elghanian R, Mucic RC, Storhoff JJ. Chemistry of oligonucleotide-gold nanoparticle conjugates. Phosphorus, Sulfur and Silicon 144 (1999): 359-362.
- [9] Reynolds AJ, Haines AH, Russell DA. Gold Glyconanoparticles for Mimics and Measurement of Metal Ion-Mediated Carbohydrate-Carbohydrate Interactions. Langmuir 22 (2006): 1156-1163.
- [10] Han G, Ghosh P, De M, Rotello VM. Drug and gene delivery using gold nanoparticles. Nanobiotechnol 3 (2007): 40-45.
- [11] Cao YC, Jin R, Nam JM, Thaxton CS, Mirkin CA. Raman Dye-Labeled Nanoparticle Probes for Proteins. J Am Chem Soc 125 (2003): 14676-14677.

- [12] Salnikov V, Lukyanenko YO, Frederick CA, Lederer WJ, Lukyanenko V. Probing the Outer Mitochondrial Membrane in Cardiac Mitochondria with Nanoparticles. Biophysical Journal 92 (2007): 1058-1071.
- [13] Thomas M, Klibanov AM. Conjugation to gold nanoparticles enhances polyethylenimine's transfer of plasmid DNA into mammalian cells. PNAS 100, 16 (2003): 9138-9143.
- [14] Hauck TS, Ghazani AA, Chan WCW. Assessing the Effect of Surface Chemistry on Gold Nanorod Uptake, Toxicity, and Gene Expression in Mammalian Cells. Small 4, 1 (2008): 153-159.
- [15] Connor EE, Mwamuka J, Gole A, Murphy CJ, Wyatt MD. Gold Nanoparticles Are Taken Up by Human Cells but Do Not Cause Acute Cytotoxicity. Small 1, 3 (2005): 325-327.
- [16] Khan JA, Pillai B, Das TK, Singh Y, Maiti S. Molecular Effects of Uptake of Gold Nanoparticles in HeLa Cells. ChemBioChem 8 (2007): 1237-1240.
- [17] DiMauro S, Schon EA. Mechanism of Disease: Mitochondrial Respiratory-Chain Diseases. The new england journal of medicine 348, 26 (2003): 2656-2668.
- [18] Piechota J, Tomecki R, Gewartowski K, Szczsny R, Dmochowska A, Kuda M, et al. Differential stability of mitochondrial mRNA in HeLa cells. Acta Biochimica Polonica 53, 1 (2006): 157-167.
- [19] Wild MD, Berner S, Suzuki H, Ramoino L, Baratoff A, Jung TA. Molecular Assembly and Self-Assembly Molecular Nanoscience for Future Technologies. Ann NY Acad Sci 1006 (2003): 291-305.
- [20] Salata O. Applications of nanoparticles in biology and medicine. Journal of Nanobiotechnology 2, 3 (2004).
- [21] Hainfeld JF, Slatkin DN, Focella TM, Smilowitz HM. Gold nanoparticles: a new X-ray contrast agent. The British Journal of Radiology 79 (2006): 248-253.
- [22] Pavlov V, Xiao Y, Shlyahovsky B, Willner I. Aptamer-Functionalized Au Nanoparticles for the Amplified Optical Detection of Thrombin. J Am Chem Soc 126 (2004): 11768-11769.
- [23] Mahtab R, Rogers JP, Murphy CJ. Protein-Sized Quantum Dot Luminescence Can Distinguish between "Straight", "Bent", and "Kinked" Oligonucleotides. J Am Chem Soc 117 (1995): 9099-9100.

- [24] Murphy CJ, Gole AM, Stone JW, Sisco PN, Alkilany AM, Goldsmith EC, et al. Gold Nanoparticles in Biology: Beyond Toxicity to Cellular Imaging. Acc Chem Res 41, 12 (2008): 1721-1730.
- [25] Daniel MC, Astruc D. Gold Nanoparticles: Assembly, Supramolecular Chemistry, Quantum-Size-Related Properties, and Applications toward Biology, Catalysis, and Nanotechnology. Chem Rev 104 (2004): 293-346.
- [26] Turkevich J, Stevenson PC, Hillier JA. A Study of the Nucleation and Growth Processes in the Synthesis of Colloidal Gold. Discussions of the Faraday Society 11 (1951): 55.
- [27] Fukumori Y, Ichikawa H. Nanoparticles for cancer therapy and diagnosis. Advanced Powder Technol 17, 1 (2006): 1-28.
- [28] West LJ, Halas NJ. Engineered Nanomaterials for Biophotonics Applications: Improving Sensing, Imaging, and Therapeutics. Annu Rev Biomed Eng 5 (2003): 285-292.
- [29] Fortina P, Kricka LJ, Surrey S, Grodzinski P. Nanobiotechnology: the promise and reality of new approaches to molecular recognition. TRENDS in Biotechnology 23, 4 (2005): 168-173.
- [30] Modified from <http://biodensing.wordpress.com/2009/06/14/gold-nanoparticles-worth-its-weight-in-gold/>. accessed on 1 July 2009.
- [31] Aillon KL, Xie Y, El-Gendy N, Berkland CJ, Forrest ML. Effects of nanomaterial physicochemical properties on in vivo toxicity. Advanced Drug Delivery Reviews 61 (2009): 457-466.
- [32] Tkachenko AG, Xie H, Coleman D, Glomm W, Ryan J, Anderson MF, et al. Multifunctional Gold Nanoparticle-Peptide Complexes for Nuclear Targeting. J Am Chem Soc 125 (2003): 4700-4710.
- [33] Tkachenko AG, Xie H, Liu Y, Coleman D, Ryan J, Glomm WR, et al. Cellular Trajectories of Peptide-Modified Gold Particle Complexes: Comparison of Nuclear Localization Signals and Peptide Transduction Domains. Bioconjugate Chem 15 (2004): 482-490.
- [34] Goodman CM, McCusker CD, Yilmaz T, Rotello VM. Toxicity of Gold Nanoparticles Functionalized with Cationic and Anionic Side Chains. Bioconjugate Chem 15, 4 (2004): 897-900.

- [35] Pernodet N, Fang X, Sun Y, Bakhtina A, Ramakrishnan A, Sokolov J, et al. Adverse Effects of Citrate/Gold Nanoparticles on Human Dermal Fibroblasts. Small 2, 6 (2006): 766-773.
- [36] Shukla R, Bansal V, Chaudhary M, Basu A, Bhonde RR, Sastry M. Biocompatibility of Gold Nanoparticles and Their Endocytotic Fate Inside the Cellular Compartment: A Microscopic Overview. Langmuir 21 (2005): 10644-10654.
- [37] Lewinski N, Colvin V, Drezek R. Cytotoxicity of Nanoparticles. Small 4, 1 (2008): 26-49.
- [38] Medda R, Jakobs S, Hell SW, Bewersdorf J. 4Pi microscopy of quantum dot-labeled cellular structures. Journal of Structural Biology 156 (2006): 517-523.
- [39] Braydich SL, Hussain S, Schlager JJ, Hofmann MC. In Vitro Cytotoxicity of Nanoparticles in Mammalian Germline Stem Cells. Toxicological Sciences 88, 2 (2005): 412-419.



ศูนย์วิทยทรัพยากร
จุฬาลงกรณ์มหาวิทยาลัย



APPENDICES

ศูนย์วิทยทรัพยากร
จุฬาลงกรณ์มหาวิทยาลัย

APPENDIX A

REAGENTS AND PREPARATIONS

1. Stock 1% hydrogen tetrachloroaurate (100 mL)

HAuCl ₄ ·3H ₂ O	1	g
Deionized water	100	mL

2. Stock 38.8 mM sodium citrate (100 mL)

C ₆ H ₅ Na ₃ O ₇ ·2H ₂ O	1.1411	g
Deionized water	100	mL

3. Phosphate buffer saline (PBS)

KCl	0.2	g
KH ₂ PO ₄	0.2	g
NaCl	8.0	g
Na ₂ HPO ₄	1.15	g

Adjust volume to 1,000 ml with distilled water and sterilize by autoclaving for 15 min at 15 psi. pH was adjusted to 7.0-7.4.

4. Dulbecco's Modified Eagle's Medium (DMEM)

Dissolve medium with 1000 mL distilled water, then 3.7 g NaHCO₃ was added to the medium and adjusted pH to 7.0-7.4. Sterilization was done using filter.

5. Freezing medium

DMEM	3	mL
Fetal bovine serum	2	mL
DMSO	0.15	mL

6. Glycine buffer

NaCl 5.84 g

Glycine 7.5 g

Adjust volume to 1,000 ml with distilled water.

7. 75% ethanol 100 ml

Absolute ethanol 75 mL

Distilled water 25 mL

8. 50X TAE buffer for agarose gel electrophoresis

Tris buffer 242.0 g

Glacial acetic acid 57.1 g

Na₂EDTA.2H₂O 37.2 g

adjust volume to 1,000 ml with distilled water.

9. 1X TAE buffer for agarose gel electrophoresis

50X TAE buffer 20 mL

Distilled water 980 mL

10. 1.5% agarose gel preparation

Agarose 0.6 g

1X TAE buffer 40 mL

11. DNA Ladder

Loading dye 20 μ L

Ladder 12 μ L

Distilled water 88 μ L

APPENDIX B

SEQUENCES OF PCR PRODUCTS

1. GAPDH sequence

ccatggcaccgtcaaggctgagaacgggaagcttgatcaatggaaatcccatcacat
cttcaggagcgagatccctccaaaatcaagtggggcgatgctggcgctgagtacgtcgt
ggagtccactggcgtcttcaccacatggag

2. ATP synthase sequence

ccatcagcctactcattcaaccaatagcctggccgtacgcctaaccgctaacattactg
caggccactactcatgcacctaattggaagcgccaccctagcaatatcaaccattaacc
ttccctctacacttatcatcttcacaattctaattctactgactatcctagaaatcgctg
tcgc

3. Cytochrome B sequence

tattcgcctacacaattctccgatccgtccctaacaaactaggaggcgtccttgccctat
tactatccatcctcatcctagcaataatccccatcctccatataatccaaacaacaagca
taatatttcgcccactaagccaatcactttattgactcctagccgcagacctcctcattc
taacctgaatcggaggacaaccagtaagct

4. Cytochrome C Oxidase 1 sequence

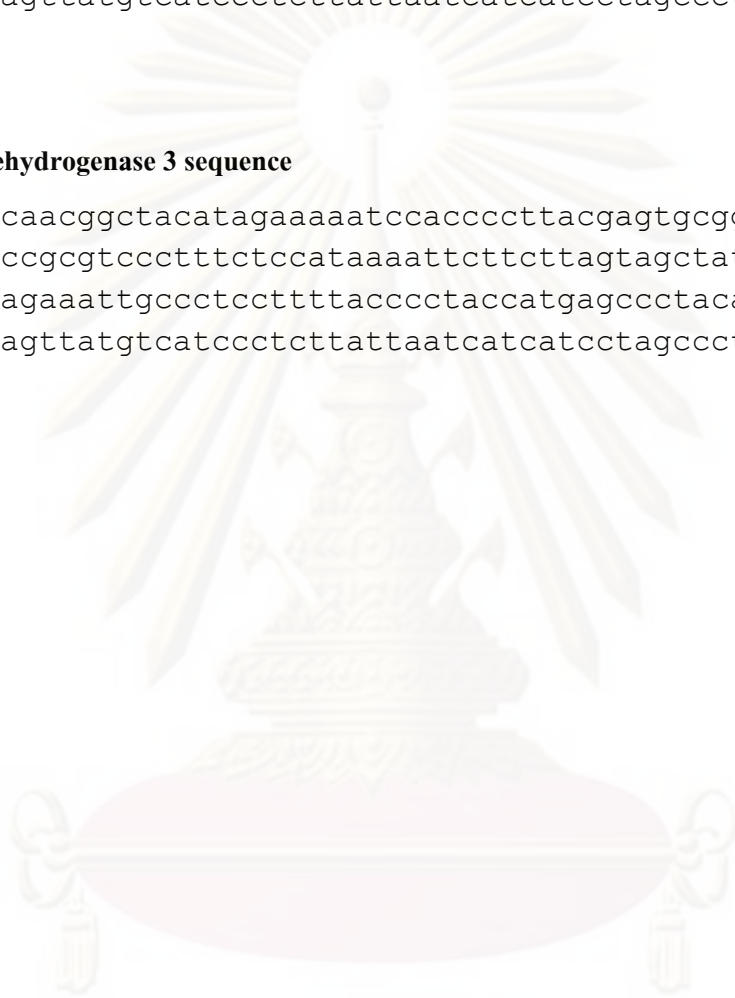
tacggtgtagcccacttccactatgtcctatcaataggagctgtatttgccatcatagga
ggcttcattcactgatttcccctatttctcaggctacaccctagaccaaactacgccaaa
atccatttcactatcatattcatcggcgtaaacttaactttcttcccacaacatttctc
ggcctatcc

5. Cytochrome C Oxidase 2 sequence

ccacaactcaacggctacatagaaaaatccacccttacgagtgcggttcgaccctata
tccccgcccgcgtccctttctccataaaattcttcttagtagctattaccttcttatta
tttgatctagaaattgcctccttttaccctaccatgagccctacaaacaactaacctg
ccactaatagttatgtcatccctcttattaatcatcatcctagccctaagtctggcctat
gagtg

6. NADH Dehydrogenase 3 sequence

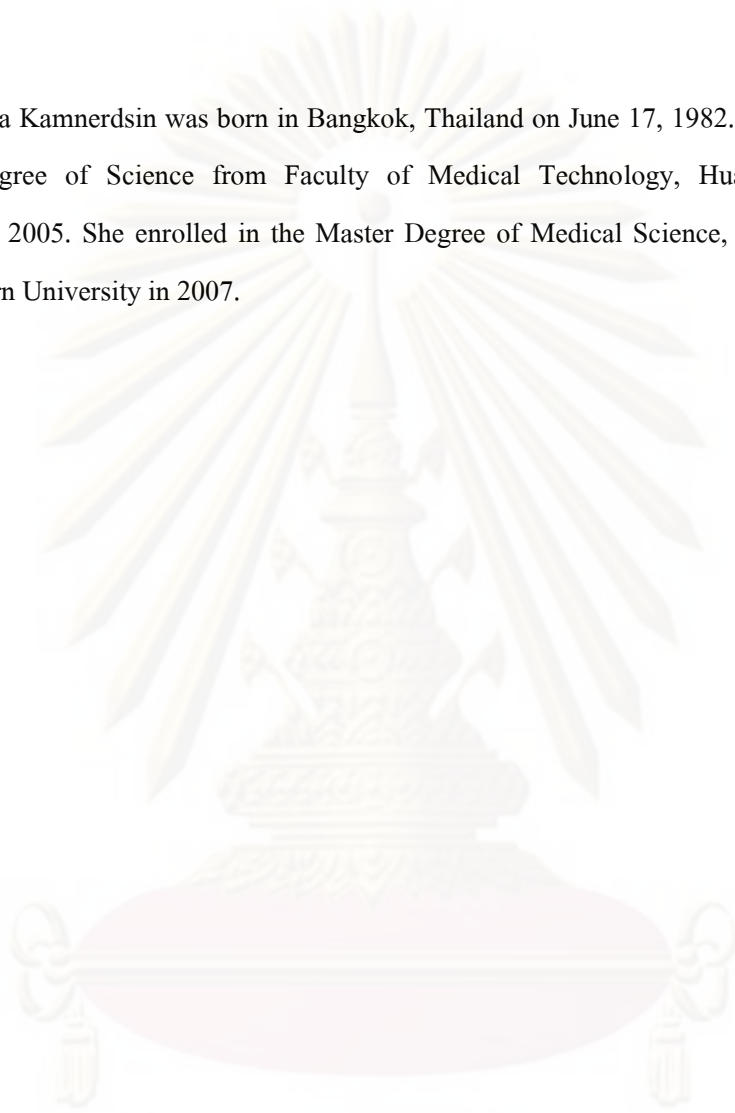
ccacaactcaacggctacatagaaaaatccacccttacgagtgcggttcgaccctata
tccccgcccgcgtccctttctccataaaattcttcttagtagctattaccttcttatta
tttgatctagaaattgcctccttttaccctaccatgagccctacaaacaactaacctg
ccactaatagttatgtcatccctcttattaatcatcatcctagccctaagtctggcctat
gagtg



ศูนย์วิทยทรัพยากร
จุฬาลงกรณ์มหาวิทยาลัย

Biography

Oraya Kamnerdsin was born in Bangkok, Thailand on June 17, 1982. She graduated with the Bachelor Degree of Science from Faculty of Medical Technology, Huachiew Chalermprakiet University in 2005. She enrolled in the Master Degree of Medical Science, Faculty of Medicine at Chulalongkorn University in 2007.



ศูนย์วิทยทรัพยากร
จุฬาลงกรณ์มหาวิทยาลัย